Quaternary International 651 (2023) 6–24

Contents lists available at ScienceDirect

Quaternary International

journal homepage: www.elsevier.com/locate/quaint

The AD 1755 Lisbon Earthquake-Tsunami: Seismic source modelling from the analysis of ESI-07 environmental data

Pablo G. Silva [a,*], Javier Elez [b], Raúl Pérez-López [c], Jorge Luis Giner-Robles [d], Pedro V. Gómez-Diego [a], Elvira Roquero [e], Miguel Ángel Rodríguez-Pascua [c], Teresa Bardají [f]

[a] Dpto. Geología, Universidad de Salamanca, Escuela Politécnica Superior de Ávila, 05003, Ávila, Spain
[b] Dpto. Geología, Universidad de Salamanca, Facultad de Ciencias, 37008, Salamanca, Spain
[c] Área Riesgos Geológicos, Instituto Geológico y Minero de España (IGME), 28003, Madrid, Spain
[d] Dpto. Geología y Geoquímica, Universidad Autónoma de Madrid, Cantoblanco, Madrid, Spain
[e] Dpto. Edafología, Escuela Ingenieros Agrónomos, Universidad Politécnica de Madrid, 28040, Madrid, Spain
[f] U.D. Geología, Universidad de Alcalá, 28871, Alcalá de Henares, Madrid, Spain

ARTICLE INFO

Keywords:
Lisbon earthquake
Earthquake environmental effects
Intensity distribution
Shakemaps
Seismic source
Iberian Peninsula

ABSTRACT

This work presents a macroseismic analysis of the AD 1755 Lisbon Earthquake-Tsunami event by means of the combination of intensity data derived from the EMS-98 scale and the ESI-07 scale (Environmental damage). About 600 records of secondary earthquake environmental effects (EEEs) for the whole Spain have been used to define intensities, focused on the SW portion of the Iberian Peninsula. The Spanish data have been complemented with 308 EEEs records from Portugal. The analyses indicate maximum intensities of X EMS-ESI along the Atlantic margin of the Iberian Peninsula with 76 records of Tsunami environmental effects (TEEs). An important amplification (VIII – VII) occurred all along the Guadalquivir basin and the adjacent Betic front at epicentral distances of 300–700 km. In these zones 55 records of ground effects (ground cracks, Liquefactions and slope movements) are catalogued. In the rest of the territory of the Peninsula the most widespread effects were hydrogeological changes with 505 records in Spain and 196 in Portugal (total 701 records) covering all the intensity levels. Increase of flow discharges in springs and elevation of water level in wells was the common groundwater response to seismic shacking, especially in SW Iberia. In this zone water elevation in wells was between 5 and 3 m and persistent increases of discharges long-lasting (several days to two months). Persistent discharges on springs were linked in 143 cases to important SW-NE crustal faults (e.g., Alentejo-Plasencia Fault). From the Intensity distribution the historic seismic scenarios are explored by means of the development of empirical ShakeMaps. These consider the three classical seismic sources proposed for this earthquake: Gorringe Bank (G); Marques de Pombal Fault (M) and Atlantic delamination beneath the Gulf of Cadiz (C). However, individually these seismic sources are too small and unable to generate the resulting seismic scenario depicted by the intensity map developed in this work, with onshore seismic accelerations (PGA) up to 0.82 g. These acceleration values and the great amplification experienced throughout the Guadalquivir basin (0.34–0.52 g) are only possible considering a combination of the three seismic sources (GMC Source) probably related to shallow subduction or lithospheric delamination beneath SW Iberia and the Gulf of Cadiz. This will suggest an NNE-SSW offshore rupture length of 350–360 km with an overall rupture area of c. 84,500 km^2 resulting in an event magnitude 8.6 Mw calculated from empirical relationships. The results demonstrate the efficacy of these kind of approaches for better identifying and modelling seismic sources for historical events.

1. Introduction

The AD 1755 Lisbon earthquake was the strongest seismic event ever reported in the Atlantic waterfront of Europe, and was extremely destructive throughout the coasts of Portugal, Spain and Morocco as a consequence of the subsequent tsunami waves (e.g., Martínez Solares, 2001; Martínez Solares and Arroyo, 2004; Baptista et al., 2003; Oliveira, 2008). Seismic shaking was felt over the whole Iberian Peninsula and far

* Corresponding author.
E-mail address: pgsilva@usal.es (P.G. Silva).

https://doi.org/10.1016/j.quaint.2021.11.006
Received 5 August 2021; Received in revised form 10 November 2021; Accepted 11 November 2021
Available online 16 November 2021

field tsunami effects were even noticed in the British islands, Netherlands, the Azores, Canary, Cape Verde islands and the Caribbean Sea (Reid, 1755). Fig. 1 shows the conventional intensity map for this event (e.g., Grandin et al., 2007) in the context of the tectonics of the Gulf of Cadiz area, which is the assumed epicentral area of this historical event. Some contemporary records compiled in a volume of the *"Philosophical Translations of the Royal Society of London"* (Robertson et al., 1755) report long period standing waves and small seiches in waters bodies located as far as the Baltic coasts of Germany, Sweden and Finland, but also apparent hydrological and hydrogeological effects in Central Europe (i.e. Switzerland and Czech Republic). Despite the numerous studies on this large historic earthquake and tsunami, there are still some important issues unsolved, such as the responsible seismic source, its dimension and the resulting earthquake magnitude (Zitellini et al., 2001; Baptista et al., 2003; Gutscher et al., 2006; Grandin et al., 2007; Martínez Solares, 2017; Fonseca, 2020; Martínez-Loriente et al., 2021). Although the seismic moment (M_o) has been obtained indirectly (e.g., Johnston, 1996; Zitellini et al., 2001; Stich et al., 2007; Pro et al., 2013) pointing to a strong magnitude of ≥8.5 Mw for this event (e.g., Mendes-Victor et al., 2010; Martínez-Loriente et al., 2021), some estimations indicate that lower magnitudes of 7.8–8.2 Mw will be sufficient to explain the event (Fonseca, 2020). More recent proposals suggest that subduction-like thrusting beneath the Horseshoe abyssal plain could account for the estimated tsunami parameters triggered by an 8.5 Mw event involving a rupture area of c. 17,000 km^2 and a minimum slip of 15 m (Martínez-Loriente et al., 2021). However, following earthquake rupture-scaling relationships (e.g., Allen and Hayes, 2017) these parameters are too small to produce earthquakes ≥8.0 Mw. At present, the rupture area, average displacement and the proper epicentral location of this event remain unclear and poorly constrained. Most of the studies appeal to complex and spatially distributed source models with thrusting at the Gorringe bank or the Horsesoe fault (e.g., Baptista et al., 2003; Mendes-Victor et al., 2010; Silva et al., 2017a; Martínez-Loriente et al., 2021) or even deep subduction beneath the Gibraltar Arc (Gutscher et al., 2006). Some other proposals also consider several rupture events offshore and onshore to explain damage distribution (Vilanova et al., 2003; Fonseca, 2020). This jumble of parametric size and location numeric data, source proposals, etc., only evidence the limited knowledge on this historical seismic event at present. As recently stated by Bufforn et al. (2020; pag. 1798): *"it is important to remember that for the Lisbon earthquake the only available data are the intensities derived from documented damages and consequently all other derived physical parameters are only estimates"*. On the other hand, except some works, most of the source proposals for this event are based on tsunami traveltime data and modelling (e.g., Baptista et al., 2003; Martínez-Loriente et al., 2021; among others) underestimating the importance of onshore intensity distribution and earthquake effects.

The present study is based on a modern macroseismic approach using building (EMS-98) and environmental (ESI-07) intensity assessments for the Iberian Peninsula. This combined analysis, focused on the SW portion of the Iberian Peninsula (mainly data from Spain), allows to build a more detailed picture of Intensity distribution for the studied zone. Aside of the large amount of EMS intensity data existing for the event in Spain and Portugal (Martínez Solares, 2001; Martínez Solares and Mezcua, 2002; Oliveira, 2008; Bufforn et al., 2020) and extensive geological evidence of tsunami records and physical models published since the 1990 decade (e.g. Andrade, 1992; Luque et al., 2002; Morales et al., 2008; Costa, 2016), analyses of onshore secondary geological effects for this event are still rare (e.g. Martínez Solares, 2001; Vaz and Zêzere, 2016; Sanz de Ojeda et al., 2019).

The present work report about 590 Earthquake Environmental Effects (EEEs) coming from the *"Catalogue of Earthquake Geological Effects in Spain"* (Silva et al., 2019a), complemented by some significant Portuguese (Oliveira, 2008; Vaz and Zêzere, 2016), Moroccan (Levret, 1755; Blanc, 1755) and global-scale EEE data (Robertson et al., 1755; Martínez Solares, 2001) achieving a total of 972 individual EEEs for the reviewed event. The study is focused on the identification, characterization, parameterization and cataloguing of the variety of Earthquake Environmental Effects (ESI-07 Macroseismic Scale) reported for Spain mainly based on the exhaustive documental analyses developed by Martínez Solares (2001) and existing EMS-98 databases. The gathered data are used to refine intensity distribution by means of the combination and discrimination of building damage EMS-98 data (Martínez Solares and López Arroyo, 2004; Martínez Solares and Mezcua, 2002; Bufforn et al., 2020) and environmental damage ESI-07 information (Gómez-Diego, 2016; Vaz and Zêzere, 2016; Silva et al., 2017a, 2019a) by the construction of a new hybrid ESI-EMS intensity map following the guidelines and applications of the ESI-07 Scale (Michetti et al., 2007; Silva et al., 2015; Serva et al., 2016; Porfido et al., 2020). This intensity map will deserve a basic tool for to check intensity patterns produced by the different possible seismic sources listed in the literature (e.g., Grandin et al., 2007) by producing maps of horizontal acceleration (PGA) following the shake-map methodology proposed by Silva et al. (2017b) for historical events.

2. Geological and geodynamic context

The Lisbon earthquake has been always associated to the geodynamic features of the Gulf of Cadiz, where complex tectonic interactions among the Atlantic oceanic crust and the Iberian continental boundary occur overriding the Africa-Eurasia Plate boundary (Fig. 1). Despite the multiple geological and geophysical research undertaken in the zone, the tectonic structure of the area and the precise seismic source of the AD 1755 event are still matter of debate (Duarte et al., 2013; Sallarès et al., 2013; Gutscher et al., 2002, 2012; Zitellini et al., 2001; Bufforn et al., 2020; Fonseca, 2020). Most accomplished models consider oceanic transpresssion along the Africa-Eurasia plate boundary controlled by geometric discontinuities in the end trace of the E-W Gloria dextral transform fault (Fig. 1). In this tectonic scenario, oceanic crustal delamination, incipient subduction or large-scale thrusting beneath the Iberian margin all along the Gulf of Cadiz zone has been proposed to explain this strong earthquake-tsunami event (e.g., Ribeiro et al., 2006; Zitellini et al., 2009; Martínez-Loriente et al., 2021). Additionally, some of these authors postulate deep eastward subduction of the Atlantic crust beneath the Gibraltar Arc as the seismic source of this historic event (Gutscher et al., 2006, 2012), identified as the "Gutscher subduction zone" in several papers (GUSZ in Fig. 1). The occurrence of these strong seismic events in the area is testified by both instrumental (AD 1969 St. *Vicente Cape Event*; Grandin et al., 2007; Bufforn et al., 2020) and paleoseismic records (218-209 BCE *Lacus Lingustinus* event; Rodríguez-Vidal et al., 2011a). This ancient earthquake occurred during the earlier roman times in the Iberian Peninsula and testified by tsunami deposits in the Doñana marshlands (Luque et al., 2002; Rodríguez-Vidal et al., 2011a), estuaries of SW Spain (Morales et al., 2008) and the Algarve coast (Costa et al., 2021). Nonetheless, at least eight similar Holocene earthquake-tsunami events are witnessed in the turbidite record around the Gulf of Cadiz (Gràcia et al., 2010).

The aforementioned tectonic scenario considers that overall transpression, crustal block rotations and delamination occurs in the Gulf of Cadiz zone generating a broad region of distributed deformation under NNW-SSE compressive stress-field (Borges et al., 2001; Buforn et al., 2004; Gutscher et al., 2012; Duarte et al., 2013; Martínez-Loriente et al., 2014). This framework caused the occurrence of a complex morphology in the ocean floor triggering eastwards thrusting and the development of NE-SW prominent structural highs (i.e. Gorringe Bank) and faults (i.e. Horseshoe and Marques de Pombal) alongside abyssal plains (Fig. 1). These NE-SW thrusting structures have been related to the instrumentally recorded strong earthquakes in the area (i.e AD 1969 7.9 Ms earthquake) and probably also with the AD 1755 event (i.e. Grandin et al., 2007; Stich et al., 2007; Pro et al., 2013; Bufforn et al., 2020; Martínez-Loriente et al., 2021). Other proposals, points to the

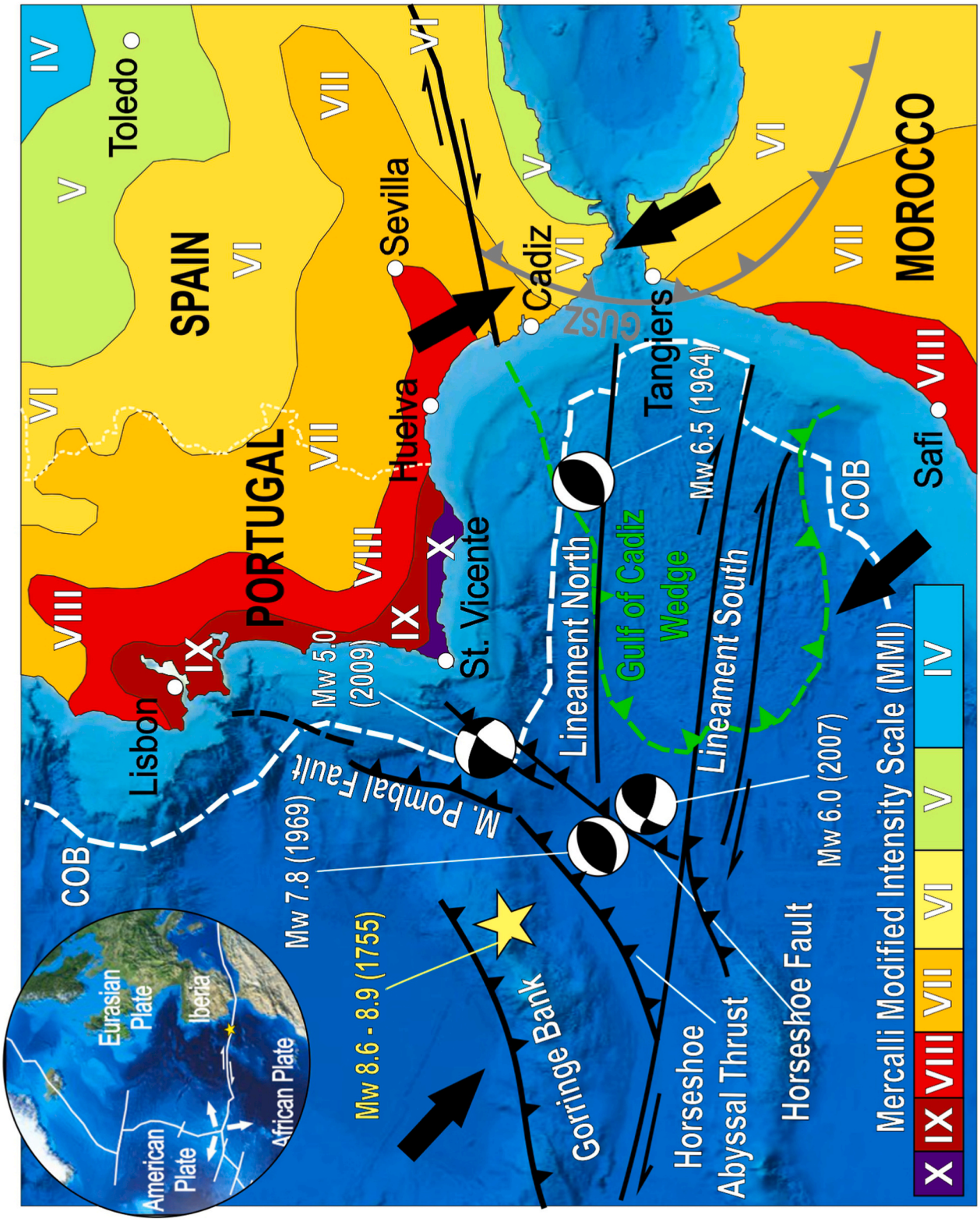

Fig. 1. Geodynamic Context of the Gulf of Cadiz in the Africa-Eurasia plate boundary (upper left inset). Faults and main tectonic structures synthetized from Duarte et al. (2011, 2013), Martínez-Loriente et al. (2014, 2021 and Gutscher et al. (2006, 2012) including the Gustcher subduction zone beneath the Gibraltar straits (GUSZ; grey shaded line) and the estimated continent-ocean boundary (COB; dashed white line) defined in Sallarès et al. (2013). Ocean floor relief from Iberpix 3.0 (Instituto Geofráfico Nacional IGN: https://www.ign.es/iberpix2/visor/). Major instrumental earthquakes (M > 6) in the zone are shown with date and focal solutions (Stich et al., 2007). Historical epicentre of the AD 1755 earthquake (yellow star) is in the Gorringe Bank following the epicentral location of this event in the Spanish IGN Catalogue (Martínez Solares and Mezcua, 2002). MMI Intensity zones in Portugal, Spain and Morocco compiled from Grandin et al. (2007). Thin dashed with line represents the Portuguese–Spanish administrative border. (For interpretation of the references to colour in this figure legend, the reader is referred to the Web version of this article.)

occurrence of accretionary wedges and eastward subduction beneath the Gibraltar Straits as possible seismic source for the AD 1755 event (Gutscher et al., 2006, 2012, Fig. 1). The lack of detail in the current knowledge of the offshore crustal structures around the Gulf of Cadiz and SW Portugal prevented more elaborate tectonophysic modelling of the probable seismic source of the Lisbon earthquake-tsunami, in particular related to the large size parameters estimated for this event. In fact, the different seismic sources proposed for this historic event are small enough to trigger a strong 8.5–8.9 Mw event as highlighted by different authors, who tentatively propose combined seismic sources (Grandin et al., 2007; Baptista et al., 2003; Silva et al., 2017a). As we will see, three different seismic sources have been proposed as the causative tectonic structures for this historic event (Fig. 1): a) Gorringe Bank; b) Marques de Pombal Fault; c) incipient eastwards subduction in the Gulf of Cadiz (GUSZ).

3. Overall features of the AD 1755 Lisbon Earthquake-Tsunami event: the global-scale effects

The AD 1755 Lisbon event is the largest historical earthquake to hit the Iberian Peninsula and the Atlantic littorals of Europe and Africa. Damage affected an area of 100,000 km^2 (≥VI EMS), with an estimated maximum local intensity of IX EMS (X MMI) in Algarve (Portugal) and VIII EMS (IX MMI) in the littoral of Huelva (SW Spain) at epicentral distances of 250–350 km (Martínez Solares, 2001). The maximum intensity is estimated in X-XI EMS at the Portuguese coast corresponding to an offshore event of magnitude 8.5–8.9 Mw (Mendes-Victor et al., 2010). The largest tsunami waves (30–35 m height) were recorded around the San Vicente Cape in SW Portugal (Baptista et al., 2003). However, this earthquake had a global extent (Fig. 2) since the earthquake was felt in an area of 10 million square kilometres (10×10^6 km^2) and its direct environmental effects, without considering tsunami effects, were observed almost 4000 km away (Martínez Solares, 2001). Fig. 2 shows a map of the global-scale earthquake secondary effects (EEEs) reported for this event. In the map six different zones are differentiated (Z0 to Z5) based on the relative seismic damage and different EEEs occurred in each one.

Z0 represents the *"Ground Zero"* of the earthquake and mainly comprises the littoral areas surrounding the oceanic epicentral area in a radius of 300–350 km severely damaged by the subsequent tsunami and listed with EMS intensity ≥ VIII in the existing literature (i.e. Mendes-Victor et al., 2010; Santos and Koshimura, 2015 and references therein). Among the most important localities within this ground zero are Lisbon, Setubal and Sagres in the Atlantic front of Iberia, Albufeira, Ayamonte, Huelva and Cadiz in the Gulf of Cadiz, Tangiers, Arcila and Safí in the Morocco coast and the Portuguese Island of Porto Santo (Madeira).

Z1 comprises those zones with significant EEEs (mainly slope movements, liquefactions, ground cracks and important hydrogeological effects) and noticeable TEEs, affected by intensities VIII - VII within a radius of c. 500 km around the epicentre. This severely affected zone includes localities such as Santarem (Portugal), Sevilla (Spain), El-Yadida and Salé-Rabat in the littoral zone of Morocco and the island of Funchal (Madeira), these last affected by damaging tsunami waves.

Z2 includes zones of intensity VI -V (limited building destruction) where noticeable EEEs occurred (mainly slope movements, liquefactions and hydrogeological effects) covering the entire Guadalquivir basin north to Sevilla (e.g. Cordoba), all the central zone of the Iberian Peninsula (Coria, Salamanca and Minateda), and SE Spain (Güévejar, Granada, Cartagena). In the Iberian Peninsula is within this zone where the most distant significant earthquake ground effects are recorded. In Africa this zone delineates a narrow strip in western Morocco including the localities of Ceuta (Spain), Marrakech, Fez and Menkes- Zerhoum (Morocco). In these last Moroccan localities important slope movements and hydrological anomalies (overflow in normally dry wadis) caused important damage (Levret, 1755). However, some historical data indicate that most of the damage occurred or was amplified due to a local earthquake (5.2 Mw - VII EMS98) occurred later on November 27, 1755 (Blanc, 1755) with intensity VII EMS98 and an estimated magnitude 5.2 Mw (Peláez et al., 2007).

Z3 comprises zones with intensity < VI where the earthquake was felt, such as the northern sector of the Iberian Peninsula (Galicia and Cantabria) as well as NE Spain (Cataluña) including the Mallorca Island in the Mediterranean. In this zone hydrogeological EEEs were massively reported, but also minor slope movements (Mallorca Island), liquefaction cases (Ebro Delta), and small tsunami effects (north Spain). A narrow strip including Melilla (Spain), Fez, Tessa and Agadir (Morocco) fringe this zone in Africa (Blanc, 1755). No more data on EEEs are reported for Africa or the Mediterranean region east of this zone that seems to terminate along the western slope of the High and Middle Atlas Mountains. To the west (Atlantic Ocean), this zone includes the Canary Islands where tsunami effects were limited, but noticeable in harbours facilities and coastal salt industries in the northern littorals of Tenerife, Lanzarote and Gran Canaria (Galindo et al., 2021). The overall data allow to assign to Z3 an approximate action radius between 800 and 1000 km (Fig. 2).

Z4 covers those regions in which the earthquake was nor felt but local anomalous EEEs were locally observed, mainly changes in turbidity and flow rate in springs (NE Spain and South France), long-period standing waves water bodies and anomalous waves in harbours and estuarine areas (far field effects). This zone covers an elliptical area of a radius between 1000 and 1800 km extended to the north, including south Ireland (Cork), the south of England (Plymouth), and the French Bretagne (Fig. 2). To the west this zone reaches the Azores archipelago, where small tsunami damage was reported (e.g. Terceira; Santos and Koshimura, 2015). This zone has been impossible to define in Africa, where documented EEEs (Levret, 1755; Blanc, 1755) only reach Z3 (Fig. 2).

Z5 delineates a very large area around the Atlantic Ocean in which far-field effects in small to large waterbodies and littoral zones (small TEEs) were locally observed (Fig. 2). In this zone there were reports of changes in temperature and the flow rate in thermal springs of France (six records), Germany (three records) and Belgium (one record), and even in the thermal baths of Töplizt in Prague (Robertson et al., 1755; Reid, 1755) about 2500 km away from the epicentre. In Germany, a new persistent thermal spring emerged in Carlstadt (Düsseldorf), plus two other anomalous variations of thermal springs around the Rhine Graben and east Germany (Sanz de Ojeda et al., 2019). In south England anomalous waves were observed in small ponds and animal watering throughs all around the counties of Cornwall, Devon, Kent, Surrey, Essex, Oxfordshire, Berkshire and Kent (Robertson et al., 1755). News from the letters sent to the Royal Society of London also indicates the occurrence of noticeable anomalous waves observed in English lakes (Cumbria, Lake district) Scottish lakes (Lomond and Ness), and Swiss lakes (Geneve, Neuchatel and Zürich) as well as in the Thames (London), Elbe (Hamburg), the Daal (Sweden) and the Aurajoki (Finland) river outlets (Fig. 2). The two last places located in the inner zone of the Baltic Sea are the most far away EEE records reported for this earthquake in Europe (Robertson et al., 1755; Reid, 1755; Oliveira, 2008). However, tsunami records (e.g. Robertson et al., 1755; Martínez Solares and López Arroyo, 2004; Oliveira, 2008; Santos and Koshimura, 2015) indicate that very minor TEE (waves of few feet) and small seiches occurred in the Caribbean zone (Barbados, Cuba), Brazil, New jersey (EEUU), Newfoundland (Canada) and even in lakes of Finland and Norway (Reid, 1755; Kvale, 1955; Mukherjee, 1755) at distances up to 6800 km away (Fig. 2). Minor sea-level oscillations occurred in the inner zone of the Caribean Sea (Central America) reported for ancient Spanish colonies in Mexico (Martínez Solares, 2017) are not indicated in Fig. 2.

Fig. 2 doesn't try to represent an intensity map, but a large-scale zonation of those areas in which EEEs and TEEs had a different size and frequency in terms of the ESI-07 Scale (observable, noticeable, significant, damaging, destructive, etc.) indicating the most

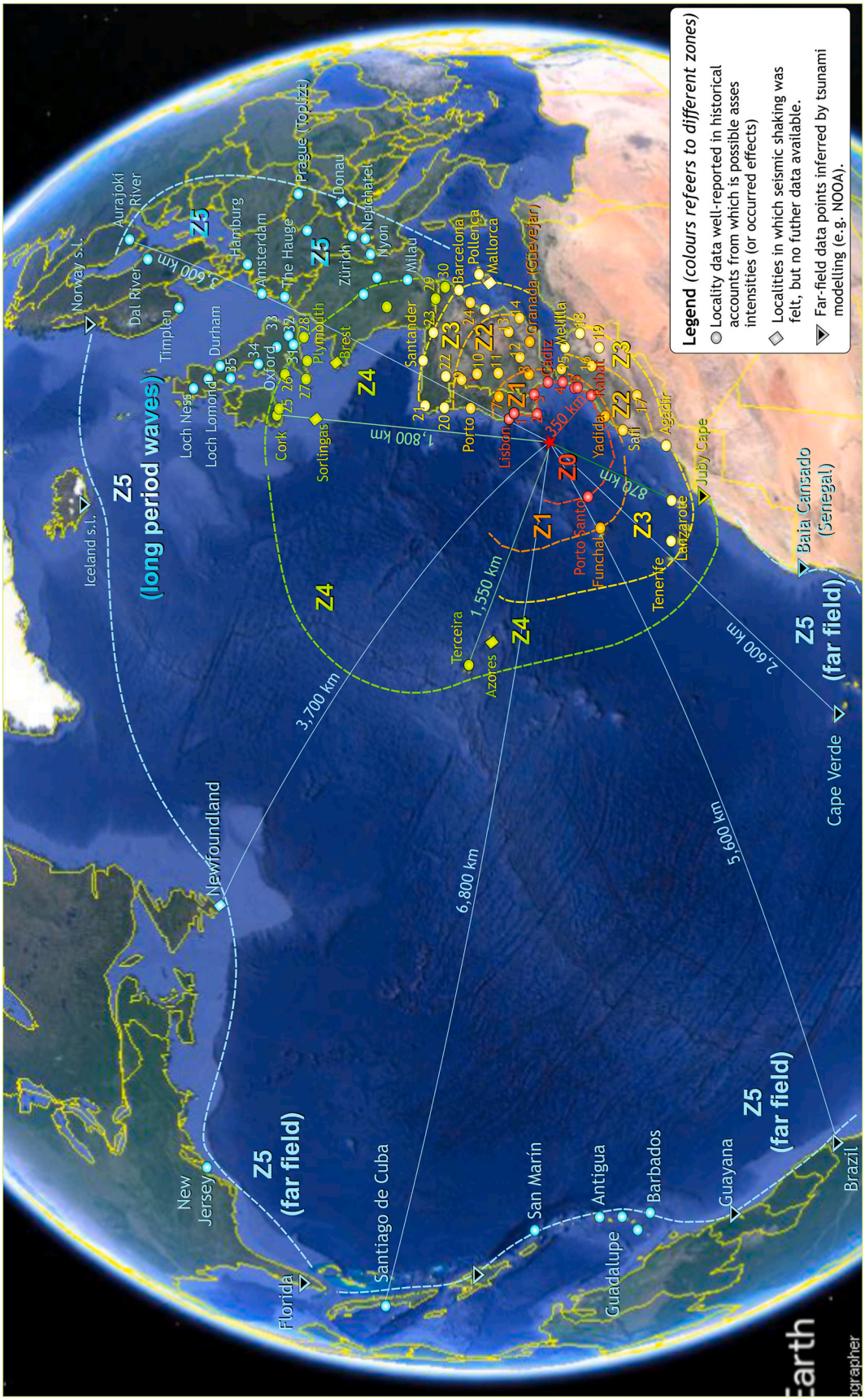

(caption on next page)

Fig. 2. Areas of different impact from the 1755 Lisbon earthquake tsunami around the globe. Aside the localities labelled in the globe map in the different earthquake affection zones. **Z0 -Ground Zero -** regions strongly affected by the earthquake and tsunami with heavy destruction (>VIII): Lisbon, Cadiz; Setubal (1); Sagres (2); Huelva (3); Tanger (4); Asilah - Larache (5), Rabat (Salé) and Porto Santo (Madeira). **Z1-**zones with large impact of earthquake shaking (relevant building destructuon) and important EEEs and noticeable tsunami effects TEEs (>VII): Santarem (7); Sevilla (8); El Yadida and Funchal (Madeira). **Z2 -** zones with moderate seismic shaking (limited building destruction) but noticeable EEEs and TEEs (VI–V): Porto; Zamora (9); Salamanca (10); Coria (11); Córdoba (12); Minateda (13) and Cartagena (14) and Güevejar-Granada; Ceuta – Tetouan (15); Menkes-Zerhoum (16); Marrakech (17). **Z3 -** areas in which seismic shaking was felt, Hydrogeological effects were massively reported, and only minor EEs and small TEEs were locally observed (<VI): Melilla; Tessa (18); Fez (19); Bayona-Tuy (20); A Coruña (21); Sanabria Lake (22); Santander, Azkoitia (23); Ebro Delta (24); Barcelona; Pollença (Mallorca island); Tenerife and Lanzarote (Canary Islands). **Z4 -** regions in which the earthquake was unnoticed but local anomalous EEEs and TEEs were observed (springs and anomalous waves in water bodies): Plymouth; Sicily Islands (Sorlingas); Cork; Kingsdale (25); Swansea (26); Penzance (27); Portsmouth (28); Le Preste-Les bains (29); Besalú (30); Terceira (Azores); **Z5 -** Large area around the Atlantic Ocean, Caribean Sea, British Isles and Central Europe in which far-field tsunami effects and long-period waves in small to large water-bodies were observed: Brest; Reading (31); Kent County (32); Essex County (33); Oxford; Chester (34); Cumbria (Lake district: 35); Durham; Loch Ness; Loch Lomond; Timplen; Daal rivermouth; Aurajoki estuary; Hamburg; Amsterdam; The Hauge; Töplizt Baths (Pargue); Donau river; Zurich; Neuchatel; Nyon (Geneve lake); Milau; Agadir; Cape Verde; Brazil; Guayana; Barbados; Guadalope; Antigua; San Marín; Santiago de Cuba; La Florida; New Jersey; Newfoundland; Iceland and Norwway coastal zones.

representative localities. All the Iberian Peninsula is included in zones ≥ Z3 and SW Iberia in Z0 and Z1 sectors, which indicate the occurrence of widespread destructive to damaging EEEs. However, the significance of Fig. 2 is to illustrate for first time in an unique map the most representative environmental effects in the far field, out of the Iberian Peninsula (sectors Z4 and specially Z5) at epicentral distances of several thousand of kilometres.

In Spain, maximum damage was recorded in the littoral of Huelva (Z0), with 66 deaths caused by the earthquake and about 1214 victims along the entire Spanish littoral of the Gulf of Cadiz (Ayamonte to Cadiz: Z1), mainly produced by subsequent tsunami waves up to 9–8 m to 3 m height (Martínez Solares, 2001). However, major damage in the Iberian Peninsula concentrated in the Atlantic coast of SW Portugal with main impact at the Algarve region and Lisbon ($Z0^{+}$), causing about 12,000 fatalities in this country, about 10,000 of them by the catastrophic destruction and the subsequent inundation of the City of Lisbon (Oliveira, 2008; Baptista et al., 2011). The total amount of victims caused by this earthquake-tsunami event was about 15,000 and 20,000, concentrated in the littoral areas of Portugal, Spain and Morocco. Economic losses have been evaluated in a total amount of about 536,000 million € (Martínez Solares and López Arroyo, 2004).

4. Methods

The analysis of earthquake environmental effects (EEs) has been performed by means of the application of the recommendations of the ESI-07 Intensity Scale following the different considered categories of earthquake effects (Michetti et al., 2007): Primary (faulting and uplift) and secondary Effects. The last includes a) Ground cracks; b) Mass Movements; c) Liquefactions; d) Hydrogeological anomalies; g) Anomalous waves and tsunamis and h) other effects. However, due to the particular characteristics of this event the hydrogeological effects have been split in two different categories related to groundwater alterations: d.1) HA; hydrogeological changes and d.2) HD: hydrogeological disturbances (Silva et al., 2019a, 2019b). The first one (HA) refers to changes in the flow rate or volume of wells, springs and fountains, including their appearance or drying (temporal or permanent). The second category (HD) consider changes in temperature, turbidity and physicochemical properties of subsurface waters. In the same way, the ESI category of "anomalous waves and tsunamis" have been also split in two, separating the tsunami effects (TEE) from other effects in surface water bodies (lakes, rivers, ponds, etc.).

The analysis of tsunami effects was undertaken by means of the application of the scale of TEE-16 (Tsunami Environmental Effects Scale; Lario et al., 2016), which represents an improvement of the ESI-07 scale in this category. The other category (WA) records anomalous hydrological effects in surface waters, such as long-period standing waves, seiches, anomalous waves in rivers, lakes and basins, appearance or drying of small lake-basins, change of the course of rivers, etc. These changes were also already applied in the *"Catalogue of Earthquake Geological Effects in Spain"* (Silva et al., 2019a). The AD 1755 Lisbon event has the particularity that it triggered all the variety of effects considered in the ESI-07 scale. Fig. 3 provide a categorized graph of the **972** EEEs catalogued for this event around the globe from exhaustive historical accounts (e.g., Robertson et al., 1755, Levret, 1755; Martínez Solares, 2001; Oliveira, 2008; Vaz and Zêzere, 2016). **905** of the EEEs (93%) are recorded in the Iberian Peninsula (**597** in Spain and **308** in Portugal), from which 76 records are tsunami effects (Santos and Koshimura, 2015).

ESI-07 Environmental Effects from Spain has been extracted, classified and catalogued from the exhaustive work of Martínez Solares (2001), who compile the letters received in the former court of the King Fernando VI from more than 1200 Spanish localities, actually preserved in the National Historical Archive of Spain. Ground effects such as slope movements (SM), ground cracks (GK) and liquefactions (LQ) in Spain have been classified and catalogued in detail (Gómez-Diego, 2016) completing 55 individual files in the Spanish Catalogue (Silva et al., 2019a). On the contrary, the categories of anomalous waves (AW), and hydrologeological effects (HA and HD) have been only classified according the ESI-07 scale and properly compared with existing EMS-98 data. The EMS-98 intensity data for the Iberian Peninsula (Spain and Portugal) and Africa (Morocco) has been taken from the on-line *"European Archive of historical Earthquake Data – AHEAD"* (https://www.emidius.eu/AHEAD). Finally, Tsunami effects (TEEs) have been reclassified following the TEE-16 Scale (Lario et al., 2016), but, since there are exhaustive papers on this subject (e.g., Santos and Koshimura, 2015) the present work does not go deeper into this topic.

The Iberian data have been implemented in a new hybrid ESI-EMS intensity map following the guidelines of the ESI-07 Scale (Fig. 3). The resulting Intensity zones were reclassified to horizontal acceleration values (PGA) following the Shakemap methodology proposed by Silva et al. (2017 b). This methodology checks the different source models proposed for this earthquake (e.g. Grandin et al., 2007; Baptista et al., 2003) applying earthquake rupture-scaling empirical relationships compiled in Allen and Hayes (2017). Similar approaches have been previously applied to other important historical or instrumental crustal events in Spain, such as the AD 1829 Torrevieja (X ESI-07), the AD 1863 Huercal-Overa or the AD 2011 Lorca (VIII ESI-07) earthquakes, produced by well-known tectonic structures (Silva et al., 2017b, 2019 b, 2020). However, for first time this methodology explores the seismic scenario triggered by a strong event with dimensions features and secondary geological effects (i.e. large tsunami waves among others) typical of subduction zone events, this is a *"subduction-like earthquake"*. The event occurred offshore the Iberian Peninsula, theoretically a passive margin (Fig. 1), but several proposals seriously consider the initiation of a subduction zone of the Atlantic crust beneath the Iberian margin in the environs of the Gulf of Cadiz (e.g., Zitellini et al., 2001; Gutscher et al., 2006; Ribeiro et al., 2006; Gutscher et al., 2012; Duarte et al., 2013, 2018). The methodological approach developed in our work allows to shed light on the probable seismic source of this event from the distribution of EEEs and TEEs in the environs of the Iberian Peninsula.

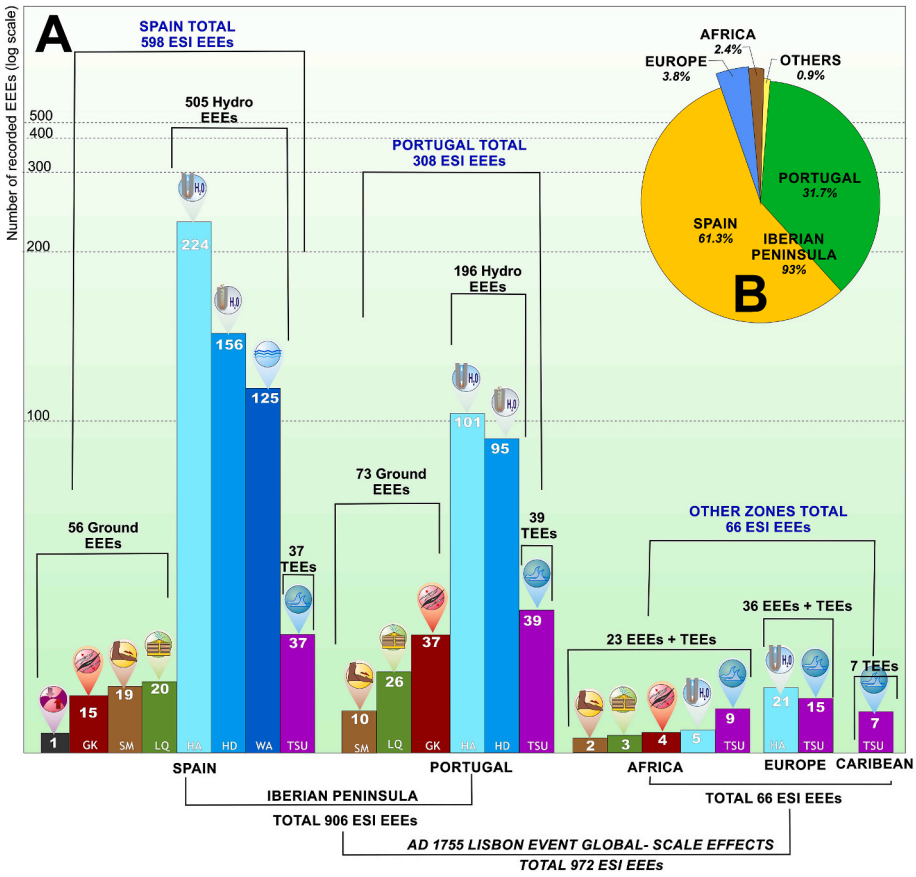

Fig. 3. A) Baar-graph showing the occurrence of the different categories of EEEs and TEEs considered in the ESI-07 scale during the AD 1755 Lisbon Earthquake-Tsunami event in different regions of the globe. B) Pie Chart showing the statistical distribution of the earthquake environmental effects in the different affected regions.

5. Earthquake ground effects

Environmental Earthquake Effects (EEE) by secondary effects covered the whole Iberian Peninsula (c. 600 × 10^3 km^2), but these mainly refers to hydrogeological changes (HA: changes in springs and wells), and disturbances (HD: variations in the chemical and/or physicochemical properties of water in wells, springs, etc.) as well as anomalous waves (WA) such as overflow or turbidity in inland surface waters. Hydrogeological effects (HA and HD) covered all the intensity levels and the whole territory of the Iberian Peninsula with 505 records in Spain and 308 records Portugal (Fig. 3). In contrast, the rest of the EEEs considered in the ESI-07 Scale, such as slope movements (SM), liquefactions (LQ) and ground cracking processes (GK) were observed in a minor amount with 56 records in Spain and 73 records in Portugal (Fig. 3). The present work analyses the EEEs occurred in Spain (Gómez-Diego, 2016). A concise analysis of those occurred in Portugal can be consulted in Vaz and Zêzere (2016). However, the implementation of the EEEs analysed by these Portuguese authors allowed in the present work the improvement of the intensity map developed by Silva et al. (2019a) only based on Spanish data and selected TEE records from Portugal (Fig. 4).

The obtained EMS98 - ESI07 hybrid intensity map, clearly reflects the impact of the tsunami on costal zones of SW Iberia, delineating a littoral fringe of Intensity X -IX (Lisboa, Algarve, to Cadiz), where additionally there are geological evidence of the tsunami impact (e.g., Luque et al., 2002; Morales et al., 2008; Lario et al., 2016; Costa, 2016). TEE data reach 76 records in the Iberian Peninsula along the mentioned littoral fringe in SW Iberia (Figs. 3 and 4). The intensity map (Fig. 4) also reveals the significant geological amplification occurred throughout the Guadalquivir Neogene basin and surrounding reliefs of the Betic Cordillera, such as the Cazorla and Segura ranges. In these zones the more important secondary ground effects (ground cracks, slope movements and liquefactions) were recorded, specifically along the southern border of the Guadalquivir basin (Fig. 4).

5.1. Primary effects: coastal subsidence

There is only one effect that can potentially be considered a primary EEE in the Iberian littoral. This is the case of coseismic subsidence at the Montegordo Beach, near the town of Ayamonte (Spain) in the Portugesse bank of the Guadiana River outlet (Fig. 5). The historical report said: "*The sea-level seems very high in this beach since* 1st *November, the ground seems to be moved in this place, no recognizable and lower. The riverbed deepened, since in those places where a small boat (canoe) could barely navigate it can now by crossed by larger sailing ships (Jabeques) with a draft (keel) of about 5 m*" (Martínez Solares, 2001). The description indicates the occurrence of probable local, but noticeable, coseismic subsidence. Ship information allow to infer at least metric-scale littoral subsidence will occur in the limit of intensity X - IX zones (Fig. 4). This site is placed c. 240 km away from the offshore location of the macroseismic epicenter considered in the Spanish official earthquake catalogue (Martínez Solares and Mezcua, 2002) (Fig. 1). Whatever the case this zone was flooded by a 10–11 m high tsunami wave (Silva et al., 2019a) and the backwash of the water will also remove or modify the topography of submerged sandy bars throughout the Guadiana outlet. Consequently, this EEE can be a false primary effect, but a significant TEE in the subtidal zone of the littoral, which can be catalogued of intensity X in the TEE-16 Scale (Lario et al., 2016). Similar reports of changes of topography in the Tagus Lagoon and river sand bars are described around Lisbon but linked to secondary ground effects or the subsequent tsunami

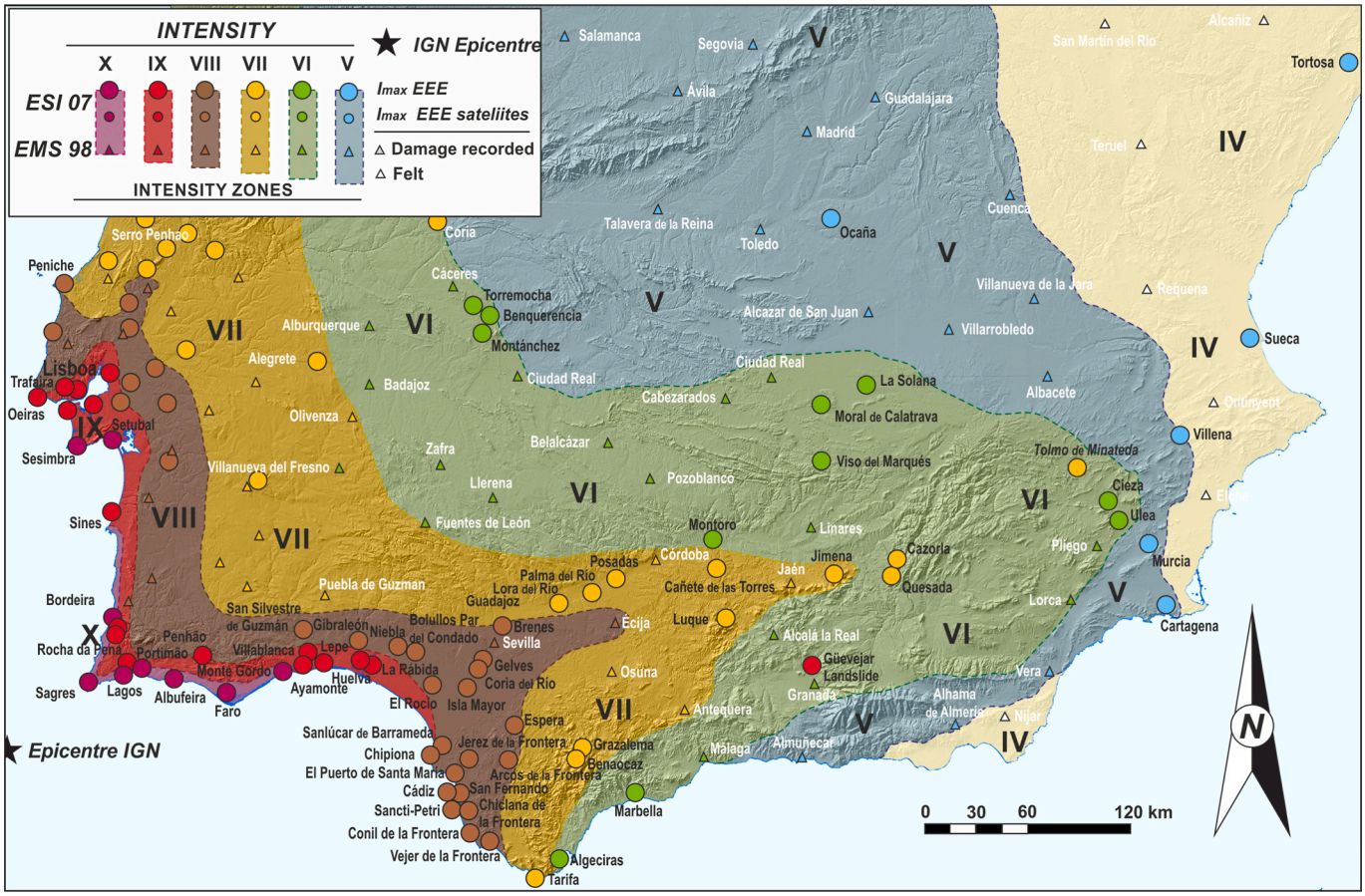

Fig. 4. Hybrid EMS-ESI Intensity Map of the AD 1755 Lisbon Earthquake-Tsunami event obtained by means the combination of macroseismic data from the EMS-98 scale (Triangles: Building damage) and the ESI-07 scale (Circles; Environmental damage). Earthquake Environmental Effects (EEEs) only include the most significant localities with ground effects such as Ground Cracks, Slope Movements and Liquefactions. Hydrological and Hydrogeological effects are excluded from this map, except for Tsunami effects classified with the TEE-16 scale (Lario et al., 2016). Map updated from Silva et al. (2019a) improved by environmental damage in the Portuguese zone compiled from Santos and Koshimura (2015) TEE and Vaz and Zêzere (2016) EEE.

action (Vilanova et al., 2003).

5.2. Secondary ground effects: ground cracks (GK)

Significant to noticeable ground cracking was observed between 200 and 300 km of epicentral distance along the littoral of El Algarve (Portugal) and Huelva (Spain). In Spain ground cracks were documented in at least 8 localities are within the intensity zones XI, VIII and VII (Figs. 4 and 5). The larger ones of centimetric width, metric to decametric length and very deep were recorded in the recent sedimentary materials of Las Antillas beach, in Lepe (264 km away). In these soft-terrains ground cracking was normally associated to the ejection of water and sands. However, the ejection of water was a common phenomenon linked to pervasive ground cracking in localities founded in crystalline Palaeozoic materials (metamorphic and granitic rocks) in SW Spain (Gómez-Diego, 2016) as is the case of the locality of San Silvestre (Huelva; Fig. 4). Centimetre-scale ground cracks were observed in rocky mountain slopes at far away localities such as Arcos de la Frontera (Cadiz) 377 km away, Luque and Cañete de las Torres (Córdoba) 523 km away or even Cartagena (Murcia) 812 km away, which is the most far EEE in this category (Fig. 5). In many cases these far-field cracks were sub-meter in width and related to unstable rocky outcrops, in other words linked to unsuccessful slope movements. On the contrary, in Portugal most of the cases of ground cracking were documented in the Cenozoic stratified deposits of the Tagus-Sado sedimentary basin (central Portugal) and few ones in the Algarve region (Fig. 5), where there are 3 of the 32 ground crack records documented in Portugal (Vaz and Zêzere, 2016). However, these authors highlight that there is an evident documentary gap on natural effects in South Portugal, where environmental damage was most extensive than documented. Consequently, many EEEs are lost in this SW sector of the Iberian Peninsula.

5.3. Secondary ground effects: slope movements (SM)

Slope movements affected an area of 35 $\times$ 10^3 km^2 in the southern half of the Iberian Peninsula. Scattered rock falls and minor earth avalanches mainly occurred in Andalucía (18 records), especially in the western mountain slopes of the Betic front area from Cadiz (Gibraltar Arc and Grazalema range) to Jaén (Cazorla - Segura ranges). This area is located at 350–650 km of epicentral distance, where the intensity was $\leq$ VII (Fig. 4). However, isolated cases of larger earth avalanches occurred within the Guadalquivir valley (in different intensity zones) linked to pronounced riverbanks or terrace scarps, where topographic susceptibility was high as is the case of the localities of Gelves in Sevilla or Montoro in Córdoba (Gómez-Diego, 2016).

Large rock falls were locally recorded at places located as far as 770 km in Albacete (Tolmo de Minateda) where slope vulnerability is important (Pérez-López et al., 2019). This site constitutes a structural butte carved in Miocene calcarenites (caprock) subject to continuous human occupation from Roman, Visigoth, Muslim, and Medieval times to the present. The site acted as a natural seismoscope recording different ancient and historical earthquakes from archaeoseismological evidence (Rodríguez Pascua et al., 2010). Regarding the AD 1755 Earthquake, historical accounts indicate: "*in the locality of Agramón, two*

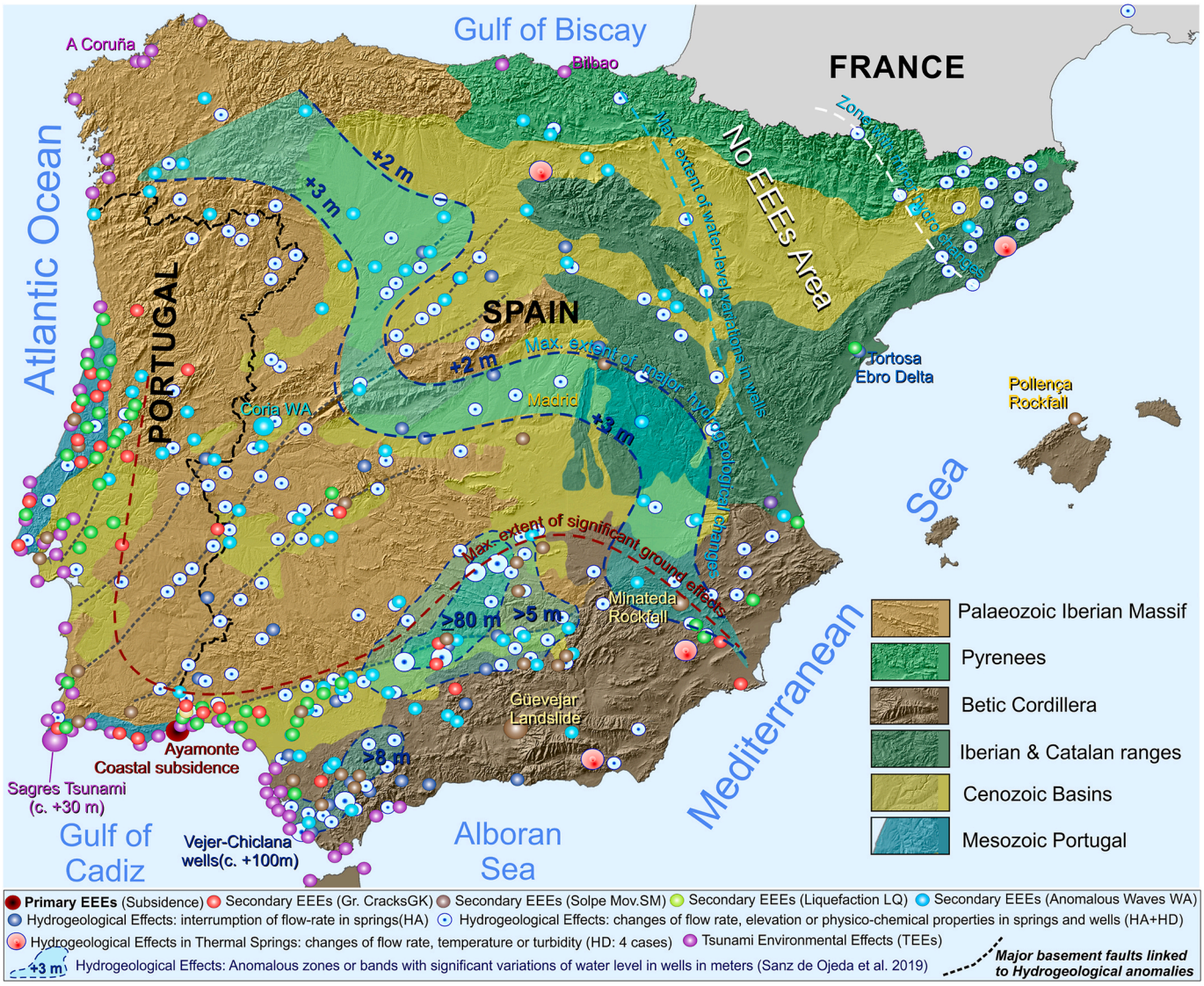

Fig. 5. General Geological Map of the Iberian Peninsula displaying the location of the more important, Ground, Hydrological (EEEs) and Tsunami (TEEs) effects triggered by the AD 1755 Lisbon Earthquake-Tsunami event in Spain and Portugal. Data from Gómez-Diego (2016), Silva et al. (2019a), Vaz and Zêzere (2016) and Sanz de Ojeda et al. (2019). Bands and zones of significant hydrogeological changes (HA) extracted from the last authors.

leagues from the town of Hellin *(Albacete Province), at the time the tremor began on the same day and hour, it was felt like a dreadful thunderclap, since a large part of a mountain collapsed without causing damage to the neighbouring farms, people or livestock"* (Martínez Solares, 2001). Research in the zone identified the Tolmo de Minateda as the "mountain" close to Agramón (6 km apart) mentioned in the historical reports. The butte displays large rock collapses along its southern scarp, with a total mobilized volume of 2300 m^3 of calcarenite blocks, with individual blocks between 50 and 1500 m^3, some of them including Visigoth carved tombs on it (Pérez-López et al., 2019). These dimensions indicate that a local intensity VII ESI-07 affected the zone (Fig. 4), clearly above intensity V or VI zones considered in previous isoseismal maps (e.g., Zitellini et al., 2001; Martínez Solares and López Arroyo, 2004). Lichenometric dating of the free-faces of the fallen blocks throw a mean age of 1733 ± 33 CE overlapping the date of the AD 1755 earthquake (Pérez-López et al., 2019).

Only an isolated large-scale landslide ~~event~~ was recorded during this event in Spain, affecting and area of c. 1,420,900 m^2 and a total mobilized rock volume of about 54 million cubic meters in the locality of Güévejar, Granada (Figs. 4 and 5; Rodríguez-Pascua et al., 2010). In this locality, 580 km away from the macroseismic epicentre, the earthquake was felt with an intensity of V-VI EMS, like that of the city of Granada, 7 km away (Martínez Solares, 2001). The landslide strongly damaged the ancient village of Güevejar, breaking down and cracking about the 93% of the houses of this locality, the church and several existing mills. 63 of 70 existing houses were seriously damaged (Jiménez Pintor and Azor, 2006), mostly due to the slow sliding of the ground surface and to the multiple ground-cracks opened within the village consequence of landsliding. The largest crack opened upslope of the locality with a semi-circular geometry of about 650 m length, 2.5 m wide and more than 10–20 m depth, which constituted the head of the landslide (Martínez Solares, 2001; Jiménez Pintor and Azor, 2006). Landsliding started about 20–24 h after the main shock, with the progressive opening of the main head-crack and a relative downslope displacement of 5.7 to 1.1 cm/h during the first ten days after the earthquake established by *in situ* measurements after the event coming from historical reports (Jiménez Pintor and Azor, 2006). The final accumulated displacement of the ground was of c. 600 m, shuttering a river valley located 1 km downslope of the village (Martínez Solares, 2001). The blocking of the valley generated a temporary lake of 5–6 m water depth, and the river course was permanently displaced several hundred meters (Gómez-Diego, 2016). Multiple cracks and fissures occurred coeval with

the landslide being also numerous the cases of apparition of new springs, as well as water and mud ejections from the largest ground cracks, being possible to classify this large slope movement as a complex rotational landslide mobilizing more than 50 million m^3 (Silva et al., 2019a). Despite the fact this site is placed within the intensity zone VI EMS-98 (Martínez Solares, 2001), ground effects point to a minimum intensity of VIII ESI-07 (Fig. 4). Parametric estimations based on the total mobilized rock volume and epicentral distance indicate that a horizontal ground acceleration (PGA) of 0.092 g was sufficient to explain the phenomena, since the marly nature and steep slope on which this locality was founded favoured site effect (Rodríguez-Pascua et al., 2010). The village was nearly abandoned after the earthquake, but formerly rebuilt at the same site. However, the landslide was catastrophically reactivated during the Arenas del Rey AD 1884 earthquake (6.9 Mw) triggering the complete destruction of the village, which was to be relocated outside the mobilized ground (Jiménez Pintor and Azor, 2006; Rodríguez-Pascua et al., 2010).

Aside of the tsunami effects in the littoral, the EEEs at Minateda and Güevejar (Figs. 5 and 6) are the two exclusive landmarks testifying permanent landscape changes within the Iberian Peninsula triggered by the AD 1755 Lisbon Earthquake. Scattered minor rockfalls occurred in other distant zones of the Iberian Peninsula between 700 and 920 km away from the epicentre (Figs. 4 and 5). This is the case of the Tajuña and Tajo Valleys (Ocaña) in Central Spain, or the Ebro Valley (Fuente Mayor; La Rioja) in Northern Spain or even in the Tramuntana range in the Mallorca Island 1220 km away (Pollença; Fontseré, 1918). Considering the ample distribution of minor rockfalls in zones of intensity $\leq$ V (Fig. 5), this type of coseismic EEE will be common within the Iberian Peninsula, but rarely documented (when no damaging).

5.4. Secondary ground effects: liquefactions (LQ)

Environmental damage for liquefaction processes affected an area about 10,000 km^2. Most of the records (at least 20 records) were widely observed along the Huelva coastal zone, the Doñana Marshlands and the Lower Guadalquivir valley (e.g. Coria, Sevilla, Brenes, etc.). These zones, between 250 and 350 km of epicentral distance, were affected by intensity VIII (Huelva zone) or VII (Guadalquivir valley and Doñana marshes zones). Most of these EEEs propagated along the Guadalquivir depression nearly delineating the intensity VII zone (Figs. 4 and 5). In the littoral zone, liquefaction originated sand volcanoes and open craterlets of few meters of diameter (Gómez-Diego, 2016). In La Rabida Convent (Huelva) explosive liquefaction occurred with the occurrence of water fountains about 7 m high (c. eight "varas"). Many other liquefaction cases occurred linked to the Guadiana, Titnto, Odial and Guadalquivir estuaries and river courses. In the Guadalquivir Depression, the liquefaction processes were mainly linked to the occurrence of large open ground cracks with the ejection of water and sands in most cases related to lateral-spreading processes. Minor cases of liquefaction occurred in floodplains of the Segura and Vinalopó rivers and littoral zones (Sueca) in SE Spain (Murcia, Alicante and Valencia) about 800–900 km away from the epicentre in zones with intensity $\leq$ VI (Figs. 4 and 5). The more distant case of liquefaction (1030 km away) occurred in Tortosa (Tarragona), close to the Ebro Delta. As in the case of ground cracks, in the Algarve region are only two catalogued cases of liquefaction possibly due to the documentary gap in the zone (Vaz and Zêzere, 2016), with most of the Portuguese documented cases of liquefaction in central Portugal (Fig. 5).

6. Secondary hydrogeological effects

Hydrogeological effects (224 HA and 156 HD) and anomalous waves in inland water bodies (125 WA) were the most widespread EEEs documented in Spain with 505 records (Martínez Solares, 2001), but also in Portugal with 196 records (Vaz and Zêzere, 2016). These anomalies affected the whole Iberian Peninsula (Figs. 3 and 5). Changes in the water level of wells (75 records) were reported for almost the three-quarter parts of Spain at epicentral distances between 260 and 925 km. In the 91% of the cases, the most common groundwater response involved the elevation of the water table in wells or increase of flow rate in springs (Sanz de Ojeda et al., 2019). A similar pattern was observed in Portuguese wells and springs (Vaz and Zêzere, 2016; Sanz de Ojeda et al., 2019). The maximum frequency of this hydrological effect was associated with the VI intensity zone (Fig. 7). Hydrogeological changes in springs also were reported for the whole Spain, even at very far away zones (1270 km of epicentral distance), where the earthquake was not felt (NE Spain and Pyrenees). The most observed effect was an increase in spring flowrates (88 records) in many cases (83 records) linked to temporal water turbidity, with most of the records between the V and VII Intensity zones (Fig. 7). The most common pattern of concatenated effects on springs was the temporal interruption of the flow (24 records) followed by the energetic recovery of the spring

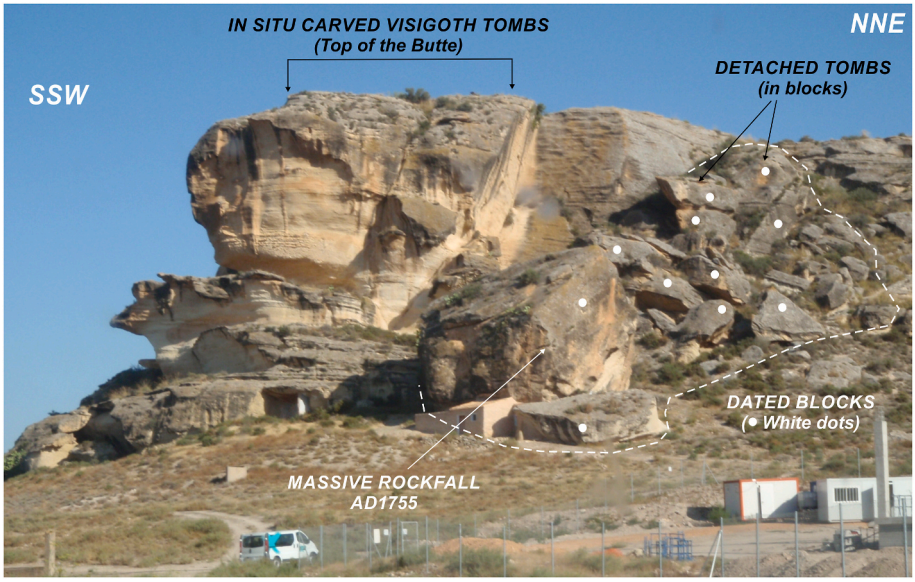

Fig. 6. Photograph of the rockfall affecting calcarenitic rocks in the "Tolmo de Minateda", displaying the position of collapsed largest blocks and carved visigothic tombs. After Pérez-López et al. (2019).

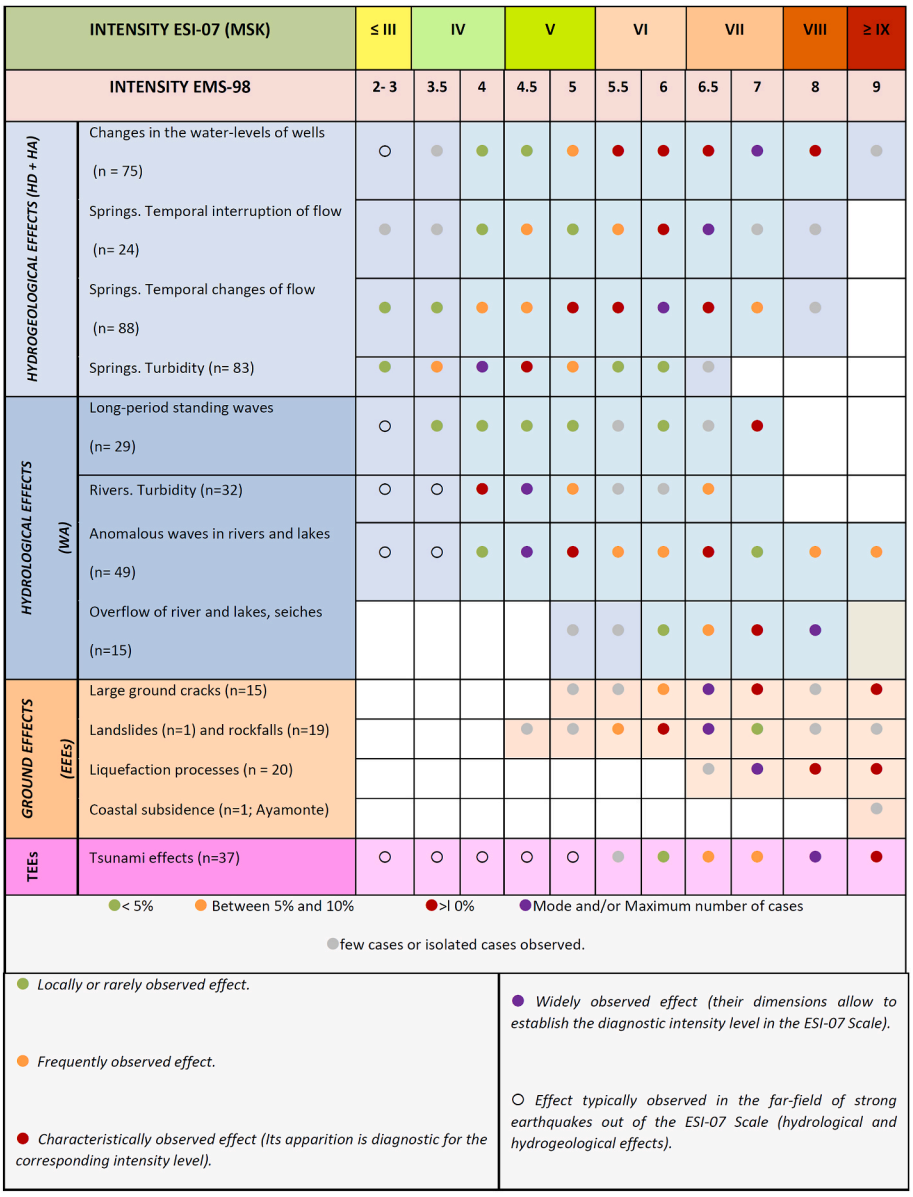

Fig. 7. Relationship between geological secondary effects (EEEs) and intensity scales EMS-98 and ESI-07 for the AD 1755 Lisbon earthquake) in Spain. Percentages of observations in relation to the total number of observations (n) of each analysed effect (based on Martínez Solares, 2001 –p. 207; Silva and Rodríguez-Pascua, 2016 – p. 99).

discharge accompanied by water turbidity (Gómez-Diego, 2016). In SW Iberia water elevation in wells was between 5 and 3 m and persistent increases of discharges were common and long-lasting, continuing from several days to two months (Sanz de Ojeda et al., 2019).

Classifying the numerical data on water-level change described in the historical accounts Sanz de Ojeda et al. (2019) perform a map of the increase of water level in wells throughout the Iberian Penninsula which master-lines are sketched in Fig. 5. In this figure is evident the undulating NW-SW strip-band crossing the Iberian Peninsula limiting the zone of significant elevation of the water-level in wells (+3-2 m). South of this band water-level rises were normally between +3 and 5 m, but two zones of anomalous upwelling were recorded in the western end of the Guadalquivir Depression at Sierra Morena (>80 m) and the Betic front in the Gibraltar Arc (>50 m). In this zone the maximum water-level increase due to the AD 1755 earthquake (c. 100 m) was recorded in the localities of Chiclana and Vejer de La Frontera, in the littoral of Cadiz (Fig. 5; Sanz de Ojeda et al., 2019). On the other hand, persistent discharges on springs were also concentrated in the southern sector of the Iberian Peninsula. In 143 cases these persistent discharges were linked to important SW-NE crustal faults (e.g., Alentejo-Plasencia or Mesejana fault) cutting the crystalline materials (granites and metamorphic rocks) of the Palaeozoic Iberian Massif. In the Duero Neogene Basin these persistent discharges also occurred in springs alongside buried SW-NE crustal faults (Sanz de Ojeda et al., 2019). These authors relate the increases in spring discharges and water-level rises to a generalized increment on groundwater pore-pressure over the whole SW Iberia caused by the earthquake.

Hydrological effects (AW) refer to alteration of rivers and lake-basins (waves, overflow, flow changes and turbidity in rivers), which were observed in most of the Spanish territory. Anomalous waves (47 records) and variations in the flowrate (26 records), accompanied by turbidity in 15 of the cases (Fig. 7), were the most observed effects. These EEEs especially occurred in the large rivers od Iberia, such as the Guadiana, Guadalquivir, Duero, Tajo and even the Miño (Fig. 5), but mainly concentrated in the Guadalquivir and Guadiana basins in SW Spain. Overflows in river courses were the most numerous effects within the

Guadalquivir River basin between the localities of Sevilla and Córdoba (Fig. 5). In Coria del Rio (Extremadura) the Alagón river eventually abandoned its course, already affected by a long-lasting process of meander chute cut-off, leaving dry the ancient medieval bridge of the locality. The historical documents indicate that progressive abandonment of the river course occurred in a long period between AD 1647 and AD 1791 due to successive floodings (Navareño Mateos, 1982), but the AD 1755 earthquake seems to set the final straw to the process. However, the abandoned stretch of the river is still occasionally swamped during important flooding events.

7. Tsunami Environmental Effects

Large tsunami waves affected the Atlantic Margin of Iberian along about 900 km of littoral between Gibraltar and Figueria da Foz (near Coimbra). Most relevant tsunami effects in Spain occurred within the intensity zones ≥ VII in an area of about 23,500 km^2 along the Atlantic coast of the Gulf of Cadiz (provinces of Huelva, Sevilla, and Cadiz; Fig. 5). There is an extensive historical documentary record of the effects of this tsunami in more than 37 sites in Spain and 39 in Portugal (Santos and Koshimura, 2015, Fig. 3), including their archipelagos (Canary and Madeira Islands). In Spain small TEEs were also observed in Galicia and several localities in the Cantabrian Sea (Martínez Solares, 2001). Historical maps, documents and geological records support the tsunamigenic interpretation of many of the sedimentary anomalous features around the Gulf of Cadiz (e.g., Baptista et al., 2003; Lario et al., 2016). Since effects of the Lisbon tsunami have been widely studied and documented by many authors, in this short section we only summarize the most relevant quantitative data around the Gulf of Cadiz in the nearest coastal zones to the offshore epicentral location.

The IGN Tsunami Catalogue assigns a Grade 6 (Ambraseys scale; Disastrous) to this event, but the application of the Tsunami Environmental Effects (TEE16) Intensity Scale results in a local maximum intensity XI (Lario et al., 2016). This means a *"Devastating Event"* with a tsunami height between 12 and 24 m, a maximum run-up of 25–40 m and an associated flooding which may penetrate few kilometres inland. This is the case of Sagres (San Vicente Cape), the nearest coastal site to the offshore epicentre (110 km away), where the height of the first wave reached a maximum of c. 30 m (Fig. 4). However, in the rest of the Portuguese Algarve shoreline the mean wave height was of 10–12 m (e.g., Baptista et al., 200) resulting in an overall intensity X. In the Spanish coast, the tsunami waves reached heights between 11 and 9 m (Ayamonte -Huelva) to 3–5 m (Cadiz) causing significant destruction along the coast (Martínez Solares, 2001; Lario et al., 2016; Silva et al., 2019a). The available data show a maximum inundation of a maximum of 5.5 km inland in lowlands and estuarine coasts of south Spain (Lario et al., 2016). Five localities were seriously damaged by the tsunami in the province of Huelva and fifteen in the Cadiz one was affected in a different extent. Important environmental effects occurred in the estuarine areas of the zone, with the record of the breaching of spit bars (Punta Umbría, El Rompido, Valdelagrana), generation of washover fans and large inundated zones with preserved tsunamites even 5 km inland (Luque et al., 2001, 2002; Morales et al., 2008; Reicherter et al., 2010). The tsunami did not go beyond the Gibraltar Strait where tsunami waves did not surpass +3 m in height (Rodríguez-Vidal et al., 2011b). The last locality with relevant tsunami damage was Conil de la Frontera (c. 350 km away), where a fishing settlement around the Conilete Tower was completely devastated and tsunami was reached up to +8 m (Lario et al., 2016). Some small sea-level fluctuations were recorded in the Mediterranean side of the Strait in the African coast, such as Tetouan or Melilla (Martínez Solares and López Arroyo, 2004).

Tsunami records allow to estimate a maximum local intensity XI in Sagres and the Algarve coast, X to IX in The Huelva littoral and VIII in the Cadiz -Tarifa zone (Figs. 4 and 5) in the TEE-16 Scale of Lario et al. (2016). As in other large tsunamis cases, zones of maximum intensities (≥VIII) at the Iberian coasts delineate a narrow littoral fringe indicating maximum run-up and inundation of the tsunami. This coastal fringe records the direct transfer of the large amount of energy released in the offshore macroseismic zone (i.e. Gorringe Bank) to the nearest coastal zones even over hundred kilometres of distance (Lario et al., 2016).

8. Results and discussion

The main results of this study are the identification and classification of the 972 EEEs reported for the AD 1755 Lisbon earthquake-tsunami worldwide (Figs. 2 and 3) as well as the proper cataloguing and parametrization within the ESI-07 scale of the 598 EEEs recorded in Spain. This data together other ground effects, tsunami damage and hydrogeological changes reported for Portugal (e.g., Santos and Koshimura, 2015; Vaz and Zêzere, 2016; Sanz de Ojeda et al., 2019) allowed a refinement on the distribution of EEEs throughout the Iberian Peninsula (Fig. 5) and a more detailed delineation of ESI-EMS hybrid intensity map (Fig. 4) for SW Spain. In a second step, this improved picture of intensity zones in the SW sector of the Iberian Peninsula is used to check different seismic scenarios explaining the obtained intensity distribution in terms of Horizontal Ground Acceleration (PGA). Since the obtained scenarios come from a hybrid ESI-EMS macroseismic approach, they are capable to explain both building and environmental damage triggered by the analysed historical event (i.e., Silva et al., 2017a).

8.1. Areal distribution of EEEs in the Iberian Peninsula

The whole Iberian Peninsula was shaken by the earthquake (583,254 km^2), ranging from the ground zero (Z0; destructive TEEs on SW littoral) to Z3 in which seismic shaking was felt and hydrogeological effects were massively reported, but only minor ground EEEs and small TEEs were locally observed (Fig. 2). Onshore EEEs were differentially distributed, and VIII to VII intensity zones clearly indicate site effects and topographic effects all along the Guadalquivir Basin and adjacent mountain areas (Fig. 4). The zone of Intensity VI encloses the area (c. 147,000 km^2) in which the most significant EEEs were observed (96%) and where more numerous ones consisted of hydrogeological changes (Fig. 7). Other hydrological anomalies, such as turbidity in rivers, springs (HD) and anomalous waves in water bodies (WA) were more numerous in zones of lower intensity (IV and V; Fig. 7).

The EEE zonation of Fig. 5 clearly displays that the south-western half of the Iberian Peninsula (c. 300,000 km^2) from Vigo (Galicia) to Cartagena (Murcia) underwent relevant hydrogeological changes (Fig. 5). Mean water increases in wells was of +2–3 m, with outsized values of even +80 to +100 m in two zones, In the same way persistent increased discharges at springs, evaluated to be between 50 and 80 m^3/s (Sanz de Ojeda et al., 2019). These authors indicate that water elevation in wells and flow rates were largely exceeded (>100 m^3/s) and more persistent in those springs linked to large crustal fractures (Fig. 5). The zone of major hydrogeological changes is limited by an undulating band nearly coincident with border of intensity zone V (Fig. 5). Beyond this undulating band hydrogeological changes, were also locally or rarely observed until but in a minor extent. A NNW-SSE theoretical line (Bilbao – Valencia) limiting the western Pyrenees and the southern sectors of the Ebro and Central Cataluña Neogene basins (NW quadrant of Iberia) limits the maximum extent of water-level variation in wells (Fig. 5) and is roughly coincident with the intensity zone IV (Fig. 4). In those areas (c. 82,000 km2) corresponding to the intensity zone III (i.e. Ebro Basin), no EEEs were reported, except one small hydrological anomaly close to the Ebro Delta (Fig. 5). On the contrary, in the more distal NW corner of the Peninsula (Fig. 5), where the earthquake was mostly not felt (intensity II), minor hydrogeological effects were reported for the province of Girona (Catalunya). These mainly consisted on turbidity in springs and long-period waves in small water bodies either natural or artificial (Martínez Solares, 2001; Gómez-Diego, 2016). Finally, it is noteworthy that the areal extension of significant secondary effects included within the isoseismal line of intensity VI is of c. 147,000 km^2 (Fig. 4) exceeding

the 10,000 km^2 considered in the ESI-07 scale for events with an epicentral intensity of XI (Michetti et al., 2007).

8.2. Checking the seismic sources proposed for the AD 1755 Lisbon earthquake: seismic scenarios

It is estimated the AD 1755 event nucleated around the Gorringe Bank in the Atlantic Ocean SW Portugal involving a variety of proposals on the probable seismic source (Fig. 1; Zitellini et al., 2001; Baptista et al., 2003; Ribeiro et al., 2006; Grandin et al., 2007; Fonseca, 2020; Martínez-Loriente et al., 2021). Most of these proposals involve the occurrence of a strong thrust-like earthquake beneath the Gorringe Bank or the Gulf of Cadiz abyssal plain, but also lithospheric delamination and incipient subduction (e.g. Gutscher et al., 2006; Martínez-Loriente et al., 2021). Among the different proposals, the Gorringe Bank (G), the Marques de Pombal Fault (M) and the lithospheric delamination and eastwards subduction of the Atlantic lithosphere beneath the Gulf of Cadiz (C) have been considered as the more probable seismic sources in the existing literature (e.g., Zitellini et al., 2001; Baptista et al., 2003; Grandin et al., 2007). As showed in Fig. 8 all these sources are compatible with the complex tectonic structuration that the present kinematics (focal solutions) exerts in this segment of the Africa-Eurasia plate boundary. More recently.

From the first studies it was clear that none of the abovementioned sources alone have a sufficient potential and dimensions (fault rupture length and area) to generate an earthquake ≥8.5 Mw as highlighted by Baptista et al. (1998, 2003) and Grandin et al. (2007). Source simulations developed by Grandin et al. (2007) signify thrusting in the Gorringe Bank (G) as the most probable seismic source for the studied event. However, some of these studies concluded that a composite source compatible with an incipient subduction along the Gorringe Bank (G) and the Portuguese margin (M) provides a better fit between onshore intensity and tsunami damage than a single source located at Gorringe Bank. In fact, a composite source linking the G and M sources will be the most suitable to explain the overall L-shaped intensity distribution displayed onshore (Figs. 1 and 4). Other studies suggest that the delamination and subduction of the Atlantic lithosphere beneath the Gulf of Cadiz (C) provides a sufficiently large seismic source capable to explain the size of the AD 1755 event (Gutscher et al., 2006, 2012; Duarte et al., 2011). This is of special importance because the occurrence of decoupling between the upper non-serpentinized and the lower mantle proposed by some authors for the zone (Sallarès et al., 2013) may favour large slips than expected during high magnitude events and consequently stronger earthquakes than expected for a single source (Silva et al., 2017).

Despite the different proposals, the seismic source of the AD 1755 event remains unclear, poorly constrained and subject of continuous debate (Fonseca, 2020; Bufforn et al., 2020). The application of magnitude – seismic source empirical scaling relationships for subduction frameworks (Allen and Hayes, 2017), indicate that each individual seismic source (G, M, C) is unable to explain the recorded intensities onshore (Silva et al., 2017a). These empirical relationships will imply rupture areas in the order of 40,000 km^2 and fault rupture lengths around 350 km and slip of 10–15 m to produce an ≥ 8.5 Mw earthquake. These numerical values are typical of large earthquake-tsunami events (i.e., Japan 2011), but all the checked sources for the AD 1755 event (G, M, C; Fig. 8) have smaller dimensions (down to 20,000 km^2) only capable to produce 7.9–8.0 Mw earthquakes (Allen and Hayes, 2017). Fig. 9 illustrates the resulting seismic scenarios produced for the three analysed seismic sources by means of the application of the shakemap

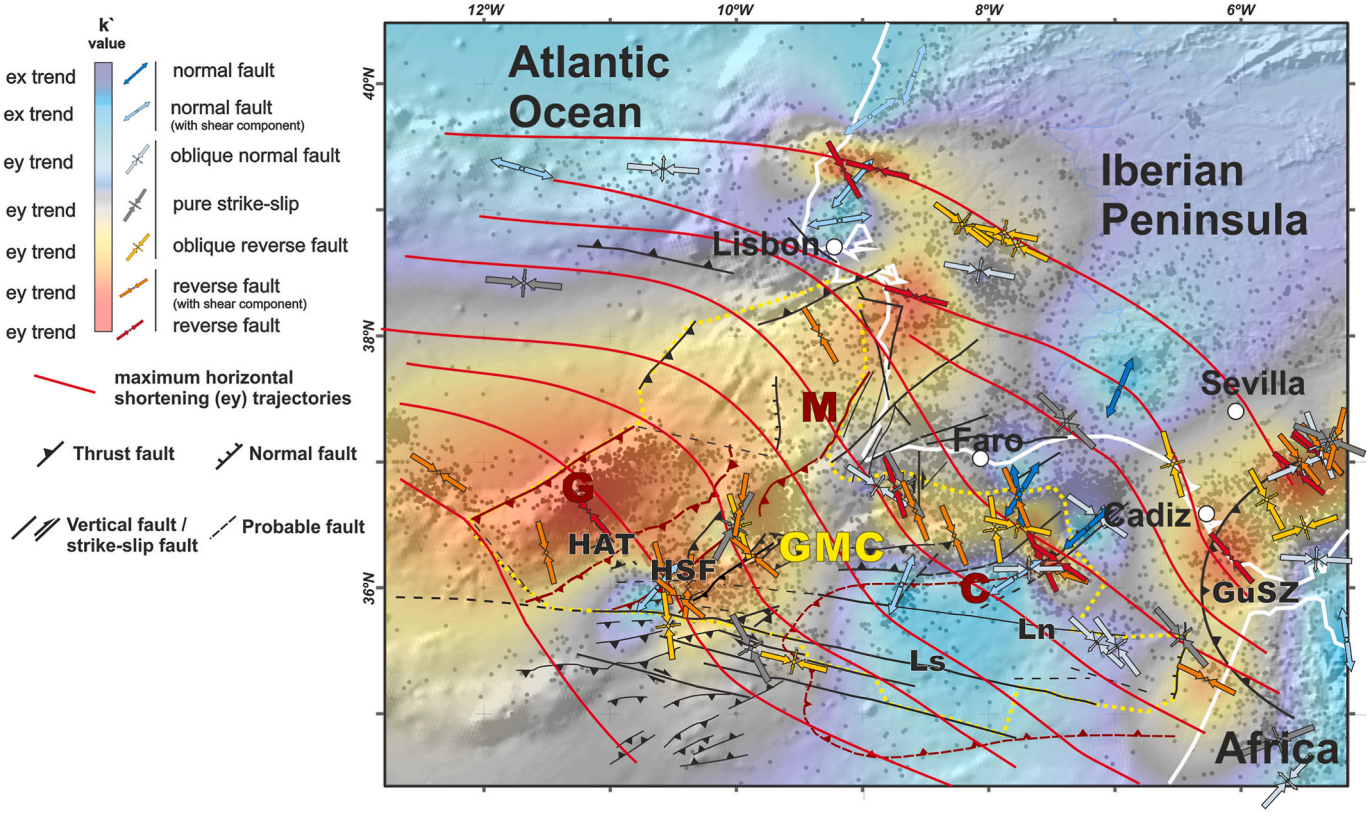

Fig. 8. Active structures in the Atlantic margin of the SW Iberian Peninsula and Gulf of Cadiz, location of the three classical seismic sources considered in the zone (G, M and C) and the composite GMC one proposed in this study (doted yellow line). Other important tectonic structures in the zone mentioned in text are also labelled: HAT (Horseshoe Abyssal Thrust); HSF (Horseshoe Fault); Ln (Lineament North); Ls (Lineament South); GUSZ (Gustcher Subduction zone). Structural data compiled from Duarte et al. (2013); Sallarès et al. (2013) and Martínez-Loriente et al. (2021). (For interpretation of the references to colour in this figure legend, the reader is referred to the Web version of this article.)

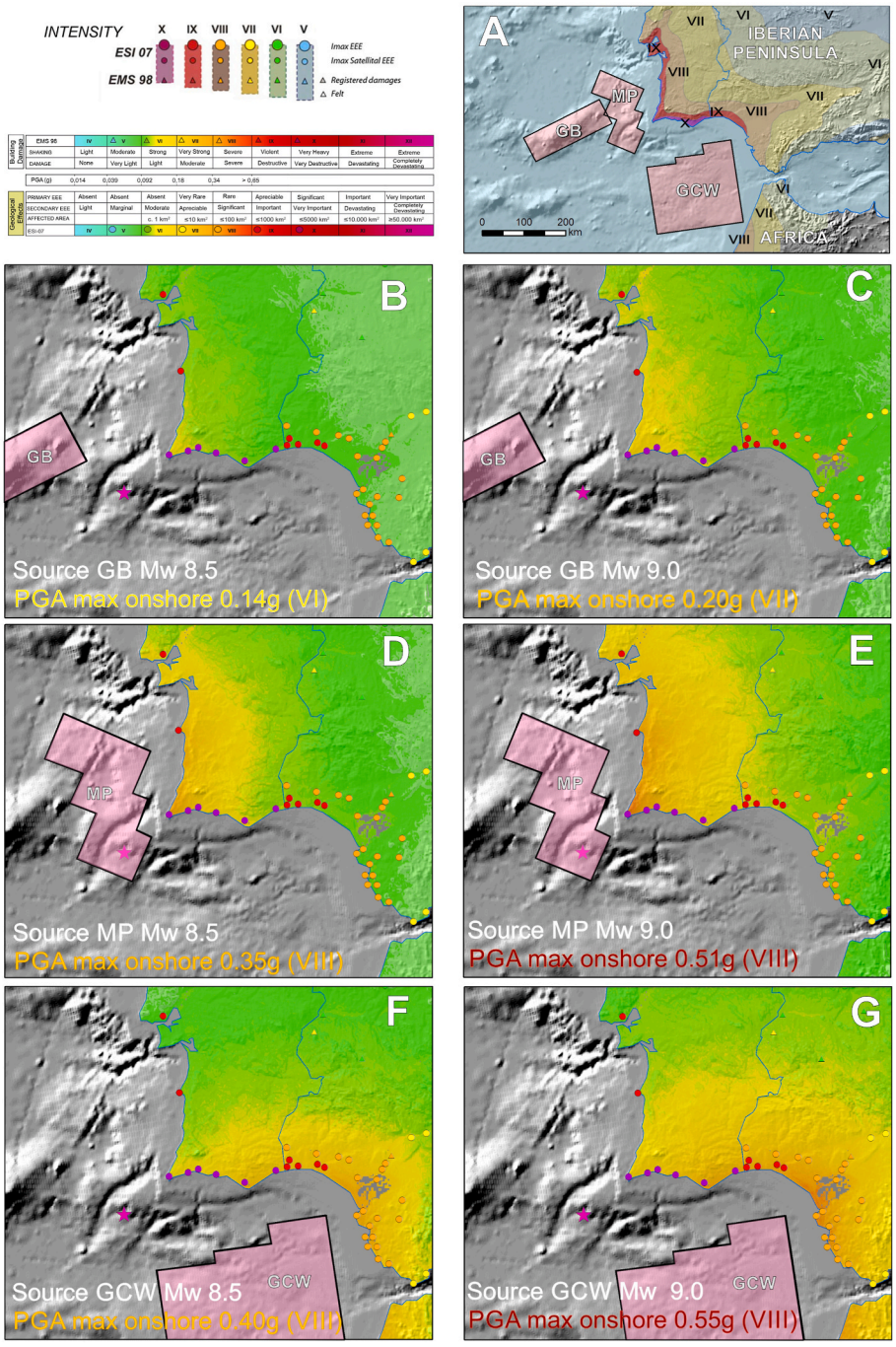

Fig. 9. Seismic sources in the SW Atlantic region of the Iberian Peninsula (G, M, C) and the computed seismic scenarios (ShakeMaps with PGA values) from the occurrence of earthquake magnitudes 8.5 Mw (B, D & F) and 9.0 Mw (C, E, G) for each individual source. Coloured dots represent intensity levels reached in selected localities in SW Iberia (See legend at top). The ShakeMaps have been produced with the methodology of Silva et al. (2017b) modified from the applied in the USGS ShakeMap Program: On-line Sahke Map Manual http://usgs.github.io/shakemap/manual_index.html.

methodology proposed by Silva et al. (2017b) for historical earthquakes. This methodology is based on (1) the production of hybrid EMS-ESI intensity maps; and (2) the selection of reliable seismic sources capable to reproduce the obtained intensity distributions in terms of ground horizontal acceleration maps. For this second step we use the ground motion prediction equation (GMP) of Boore et al. (1997) widely applied in the USGS ShakeMap Program (Wald et al., 2005). However, the USGS methodology was corrected by incorporating into the equations the topographical and geological correction factors proposed by Silva et al. (2017b). This correction factors specially improved the estimations of ground acceleration values across the Guadalquivir Basin and adjacent mountain borders.

In the three checked cases (G, M, C), 8.5 Mw or 9.0 Mw earthquakes have not enough size to reproduce the large intensities reached onshore (Fig. 9). Only source C has the minimum dimensions to generate a c. 9.0 Mw earthquake following the used empirical relationships. The computed PGA values at coastal sites are down to 0.40–0.55 g for source C, implying maximum EMS-ESI hybrid intensities of VIII in the Iberian littoral (Fig. 9F and G). Sources G (0.14–20 g) and M (0.35–0.51 g) result in still lower PGA values only capable to generate intensities VII or VI at coastal sites (Fig.9B to E). The maximum seismic scenario for source C (Fig. 9C) would imply the record of PGA max values around 0.55 g, in the upper range of intensity VIII, along the southern Iberian littoral. Even in this case, computed PGA values around Lisbon (0.12 g) will not go beyond intensity V, and those for the Guadalquivir Depression upstream Sevilla hardly reach values related to intensity VI (0.19–0.21 g; Fig. 9G).

8.3. Checking a new composite seismic source compatible with the seismotectonic and structural framework of the Gulf of Cadiz

All the checked cases result in undersized acceleration values compared with the intensities recorded onshore (Fig. 9). Considering the obtained results, it seems clear that an 8.5–9.0 Mw event in the zone will need a seismic source of larger dimensions. Recent tectonic proposals for the SW Iberian Margin indicate the probability of the occurrence of an extensive composite or multiple seismic source (G + M + C) linked to thrusting and eastwards delamination or incipient subduction of the Atlantic lithosphere (Zitellini et al., 2009: Gutscher et al., 2012; Duarte et al., 2013; Martínez-Loriente et al., 2014, 2021; Silva et al., 2017). Some of these authors assume that the Gulf of Cadiz zone is a similar case to those recorded in the Lesser Antilles and Scotia subduction arches in the opposite margin of the Atlantic Ocean (e.g., Duarte et al., 2018). From these tectonic proposals and regional structural data of the SW Iberian margin a new composite seismic source has been modelled for this work as preliminary suggested by Silva et al. (2017a). The composite seismic source proposed here will include thrusting along the NE-SW linear structures of the Gorringe Bank (G) and Marques de Pombal Fault (M) and low angle delamination (*decollement)* of the Atlantic lithosphere beneath the frontal accretionary wedge of the Gibraltar Arc (C) in the Horseshoe abyssal plain (Fig. 8). To the south this structure will be limited by one of the important right-lateral faults subject to wrench tectonics in the zone, the so-called South Lineament fault (Duarte et al., 2011, 2013). This fault, together the Horseshoe fault are considered to be among the most active tectonic structures in the zone (Silva et al., 2017) and capable to generate strong earthquakes, such as the Lisbon one (Martínez-Loriente et al., 2018; 2021; Serra et al., 2018). In detail, the geometry of eastern limit of the proposed seismic source fairly replicates the contact of the different lithospheric domains present in the Gulf of Cadiz area delineated by Sallarès et al. (2013).

To check the geodynamic model related to the proposed seismic source the *"ey trajectories"* (maximum horizontal deformation: *SHmax*) and the related *"k coefficients"* (strain tensor shape factor) have been calculated for the zone. The performed stress map (Fig. 8) is based on the analysis on available focal solutions of instrumental seismicity (grey dots) in the zone between the years 2000 and 2015. The kinematic analysis comes from the stress inversion of "*earthquake focal solutions"* which allows to define a stress regime based on the spatial orientation (trend and plunge) of the obtained P and T axis (e.g. Capote et al., 1991; Müller et al., 1992) and largely applied in the Iberian Peninsula, Europe, the Atlantic basin margins (De Vicente et al., 2008; Olaiz et al., 2009; Giner-Robles et al., 2009), as well as in the world stress map project (Heidbach et al., 2018). The interpolation of the multiple *"ey data"* (arrows) calculated for individual focal solutions enables to map the *SHmax* trajectories array (*ey* lines in Fig. 8) as well as to calculate the related *"k coefficients"*. This workflow results in maps of the strain tensor shape, which is expressed as background-coloured sectors from pure compressional (red) to pure extensional (blue) tensors (Fig. 8) following the methodology proposed by Giner-Robles et al. (2009).

The obtained *ey* trajectories are compatible with the proposed ESE large-scale thrusting source mechanism (GMC). The *k factor* (*strain-tensor shape)* shows as active compression are clearly related to the initiation (G and M sources) of the proposed composite seismic source, where reverse and oblique reverse focal solutions are abundant (Fig. 8). Similar compressive stress fields dominate the Atlantic margin of Iberia south of Lisbon and the Algrave zone bounding the proposed composite zone to the North. However, in the central zone of the Gulf of Cadiz blue extensional sectors are dominant and compression only becomes relevant again around the Gibraltar Arc (Fig. 8) The near absence of *ey data* (arrows) to the West (G and M) and South (Ls) of the proposed composite source is due to the lack of instrumental seismicity in these zones (Fig. 8). These active structures apparently seem to be either locked or moving aseismically at present and only will undergo frictional slip during high magnitude earthquakes, triggering stronger earthquakes than expected as proposed by Silva et al. (2017). These authors also identify important microseismic ($\leq$4.5 mb) activity east to the HSF, which other authors interpret as large-scale thrusting of the serpentinized upper mantle beneath the Gulf of Cadiz Abyssal Plain (e.g. Martínez-Loriente et al., 2021).

The proposed seismic source has a potential rupture area of c. 84,500 km^2 and a potential rupture length of 357 km along the NE-SW faults bounding the Gorringe Bank and northern structures (Fig. 8). Considering these geometric parameters, empirical relationships for offshore events (Allen and Hayes., 2017) indicate that the proposed source will trigger an earthquake of maximum magnitude between 8.6 and 8.7 Mw. These values agree with the widely accepted magnitudes proposed for the AD 1755 event (i.e., Bufforn et al., 2020). To check the theoretical intensities and PGA values related to this earthquake magnitude produced by the proposed composite seismic source (GMC), a last seismic scenario is calculated (Fig. 10). The obtained results match reasonably with the recorded intensities all along the SW quadrant of the Iberian Peninsula illustrated in the classical isoseismal maps (Figs. 1 and 10). Maximum intensities (X) occur in the Algarve littoral with computed PGA values between 1.15 g and 0.85 g from Sagres (St. Vicente Cape) to Faro. In the Gulf of Cadiz PGA values decrease from west (Ayamonte; 0,65 g) to east (Doñana marshlands; 0.45 g) supporting intensities between IX and VIII along the coast. Towards the Gibraltar Arc, the city of Cadiz (0.34 g) is within the transition from intensity VII to VIII (Fig. 10). To the north along the Portuguese coast the PGA values indicate intensity values between X and IX. Lisbon reaches a computed PGA of 0.76 g supporting a minimum intensity of IX as in the classical intensity models (Martínez Solares and López Arroyo, 2004). The computed model also describes well the amplification to intensity VIII –VII recorded within the Guadalquivir Basin (Sevilla 0.33 g; Córdoba 0.21 g) as well as intensities $\geq$ V recorded in the great part of SW Iberia (Fig. 4).

The need of a large source area has been demonstrated previously (e.g., Johnston, 1996; Zitellini et al., 2001) and the fact that sources M and G are not sufficient to release the needed energy was also already discussed by Baptista et al. (2003), Grandin et al. (2007) and Martínez Solares (2001). The proposed composite source (GMC) agrees with energy considerations, available intensity data and produces a quite good fit of the obtained isoseismal distribution (Fig. 5). This composite source will agree with the anomalous duration of the ground shaking (6–7 min) reported as three shocks separated by two intervals of a couple of minutes (Reid, 1755; Martinez-Solares, 2001; Vilanova et al., 2003). In fact, a nearly simultaneous rupture of different sources around the Gulf of Cadiz. This would not necessarily to imply the presence of an accommodation east-dipping surface (decollement) connecting the faults at depth between 16 and 18 km (e.g. Gutscher et al. (2012). However, recent geophysical data (Silva et al., 2017; Martínez-Loriente et al., 2018, 2021) identify a deep thrust fault located beneath the Horseshoe Abyssal plain (HAT) probably connecting with the decollement levels under the Gorringe Bank, which will be included in the extended seismic source proposed in this paper (Fig. 5). Nevertheless, depth geometrical parameters are not considered in the ShakeMap procedures used here (Silva et al., 2017b). According to Duarte et al. (2013) and Sallarès et al. (2013) NNE–SSW to N–S westerly dipping thrusts in the southwest slope of Iberia accommodate W-E to NW-SE shortening, which indicates that westward directed thrusting propagates from the Gibraltar Arc to the west and to the north along the Portuguese margin (i.e. Marques de Pombal Fault) and Horseshoe abyssal plain (e.g. Silva et al., 2017; Martínez-Loriente et al., 2018). To the south the NW movement of the African plate generates strain partitioning by means of dextral wrenching on WNW–ESE trending steep faults (Duarte et al., 2011) delimiting the southern border of the proposed extended source (Figs. 8 and 10) and thrusting on the NE–SW trending fault in the Gulf of Cadiz and Horseshoe Abyssal Plain. In detail, the proposed composite seismic source roughly coincides.

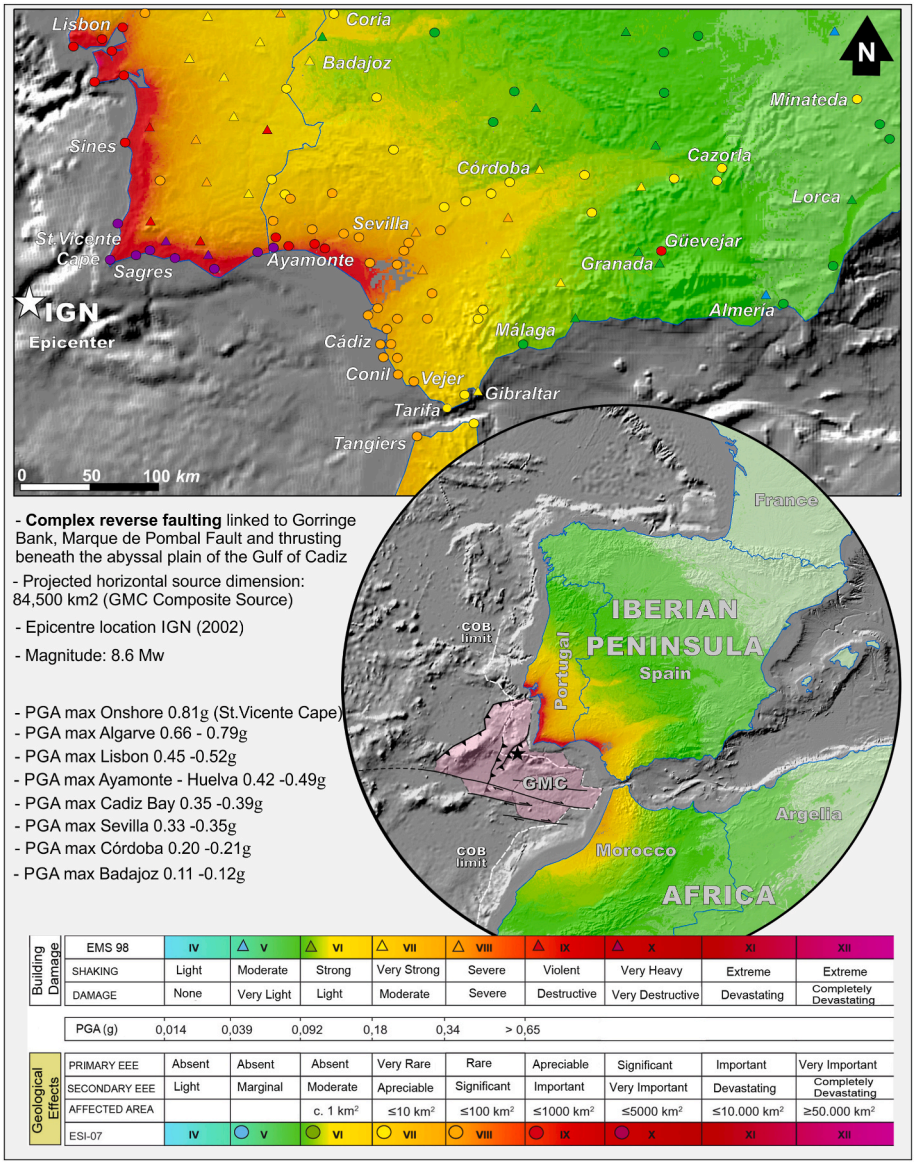

Fig. 10. ShakeMap for the AD 1755 Lisbon earthquake produced by the composite seismic source GMC proposed in this study.

9. Conclusions

This study gathers and classifies the large amount (972 records) of Earthquake Environmental Effects consequence of the AD 1755 Lisbon Event at global scale (Fig. 3), providing an original picture of the earthquake on different continents (Fig. 2). Tsunami effects (TEEs) were recorded at distances as far as 5600–6800 km in the opposite side of the Atlantic Ocean. Hydrogeological EEEs was the more widespread recorded effects both in the Iberian Peninsula (701 records) and the rest of Europe, including the British islands, with 727 global records at maximum distances of c, 2000 km (Teplitz Baths; Chez Republic). 505 hydrogeological EEEs records occurred in Spain, the c. 70% of them in the SW sector of the Iberian Peninsula (Figs. 3 and 5). Ground EEEs were only documented within the Iberian Peninsula and few in North Africa at epicentral distances down to 500 km (Fig. 2), with 56 records in Spain and 79 in Portugal (Fig. 3). The most common ground EEEs in Spain were ground cracks (15 records), liquefaction (19 records) and slope movements (20 records), which are the properly catalogued ones.

The analysis of EEEs records in SW Spain and Portugal (Fig. 5) allowed to elaborate a hybrid ESI07 – EMS98 intensity map (Fig. 4) combining building damage data coming from the existing seismic data bases (e.g. AHEAD Program). The study illustrates that the classically accepted seismic sources for the AD 1755 Lisbon event (Fig. 1) cannot individually explain on their own the intensity distribution caused by this earthquake (Fig. 9). The seismic scenarios (ShakeMaps) obtained for these sources indicate that they are too small to produce or explain intensity levels (or PGA values) reached in the Guadalquivir basin and in the Gibraltar Arc. Solutions based on the subduction beneath the Gulf of Cadiz alone (C) provide very good intensity constraints for the southern Spanish littoral and the Guadalquivir basin but are still insufficient to explain the intensity levels reached around the Portuguese littoral and Lisbon area to the north. Following the tectonic models for the zone (Duarte et al., 2013; Sallarès et al., 2013; Martínez-Loriente et al., 2014, 2021), we propose a composite seismic source including all the three traditionally considered sources (Fig. 10; GMC) in a process of incipient eastwards subduction (lithospheric delamination or thrusting) of the Atlantic lithosphere beneath the Gulf of Cadiz. In fact, the geometry of the western boundary of the proposed source can be adapted to the continent-ocean crustal transition proposed for the Gulf of Cadiz area (Sallarès et al., 2013).

The proposed seismic scenario fulfils the intensity distribution recorded across the whole Iberian Peninsula in terms of seismic

acceleration values (PGA), but also the large source geometric parameters required to generate this kind of strong events. This scenario also supports the classical L-shaped geometry of stronger intensity levels (IX – X) between Lisbon and the Doñana Marshlands combining EMS-98 and ESI-07 data. In terms of reliability, the proposed source can be another possible seismic source for the studied event, but in this case deeply rooted in a detailed macroseismic analysis of earthquake environmental damage inland and offshore. In this point is important to remember that for the Lisbon earthquake the only available data are the *"intensities obtained from documented damages and consequently all derived parameters are only estimates"* (Bufforn et al., 2020). Whatever the case, the origin of the Lisbon Earthquake will continue to be challenging since it is an intensity X historical subduction-like event produced in a theoretically passive margin.

The question of the unusual long duration of the earthquake (6–7 min) and its perception as three individual shocks separated by a few minutes (e.g. Reid, 1755) raises the possibility of the occurrence three nearly simultaneous earthquakes around the Gulf of Cadiz. The Indian Ocean earthquakes of 2011, separated by c. 2 h and a few hundred kilometres, had magnitudes Mw 8.6 and Mw 8.2 and was consequence of different multiple fault ruptures (Wang et al., 2012). A similar case was the Mw 9.0 Tohoku event in the Japanese subduction zone, which resulted of a complex rupture slip-model featured by three shock pulses separated by few seconds with a total duration of 6 min (Koketsu et al., 2012). If both events would be damaging historical earthquakes, we would probably be bundling together the macroseismic data obtaining a larger magnitude. Spatially distributed and multiple rupture sources are proposed by Fonseca (2020) to explain earthquakes with abnormally long duration of ground shaking, as is the case of the AD 1755 Lisbon event. In our case, the test for the individual seismic sources displayed in Fig. 9 indicates that if closely time-spaced multiple rupture occurred minimum magnitudes of each one will be of at least 8.5 Mw. However, much more geological data will be necessary to unravel the true source of this earthquake.

On the other hand, The Lisbon event produced much more far field effects, especially hydrogeological changes and seiches, than those documented for recent strong earthquakes ($\geq$8.5 Mw), such as the case of the 2004 Indonesian or the 2011 Tohoku (Japan) subduction events. Despite the great GPS coverage of far-field ground displacements available for the 2011 Tohoku earthquake (e.g., Wang et al., 2011), data on ground and hydrogeological EEEs are scarce and only restricted to the Japan island at epicentral distances down to 300 km (e.g., Yamaguchin et al., 2012; Sánchez and Maldonado, 2016) as widely occurs at this distance range in events of magnitude $\geq$6.0 Mw and intensities $\geq$ VIII (e.g. Muir-Wood and King, 1993; Esposito et al., 2001). On the contrary, the AD 1950 Assam earthquake (8.6 Mw) produced small seiches in lakes of Britain, Ireland and Norway at epicentral distances up to 7500–8000 km (e.g., Kvale, 1955), but no similar records have been published for the Indonesian or Japanese events. It seems that the progressive seismic and remote sensing instrumentalization throughout the 20th century resulted in a devaluation of intensity records and especially of those concerning earthquake natural effects in the far-field. Hopefully, since the ratification of the ESI-07 Scale recent earthquakes are again subject of deeper geological research and reports on EEEs are gaining attention (e.g., Serva et al., 2016; Porfido et al., 2020 and references therein). Whatever the case, the AD 1755 Lisbon Earthquake shows very specific far-field features and will continue to be a rare and singular global-scale event subject of debate.

Author contributions

Pablo G. Silva (PGS): Conceptualization, Investigation, Methodology, Coordination, Writing and original draft preparation, Conclusions and figures, Contribution in data acquisition. **Javier Elez** (JEZ): Investigation, Methodology, Formal analysis, Imagery management, ShakeMap processing, Figures, Review. **Raúl Pérez-López** (RPL): Investigation, landslides analyses, Seismotectonics, Contribution in data acquisition, Review and editing; **Jorge L. Giner-Robles** (JLGR): Investigation, Seismotectonics and MAT earthquake analysis, review and figures. **Pedro V. Gómez-Diego** (PVGD): investigation, Formal analysis, Data base management, kmz files, Analysis of historical data, Contribution in data acquisition. **Elvira Roquero** (ERQ): Formal analysis, Analysis of historical data, Contribution in data acquisition. **Miguel A. Rodríguez-Pascua** (MARP): investigation, Formal analysis. **Teresa Bardají** (TBA): investigation, Formal analysis, Tsunami data, Review and editing. All authors have read and agreed to the published version of the manuscript.

Data availability

Individual files for EEE Spanish data discussed in this study are described in detail in the "2nd Edition of the Catalogo de Efectos Geológicos de los Terremotos en España", published by the Spanish Geological Survey in 2019. The Catalogue is openly available at:

https://www.igme.es/Publicaciones/publiFree/Cat%C3%A1logo%20de%20efectos%20geol%C3%B3gicos%20de%20los%20terremotos%20en%20Espa%C3%B1a/index.html (Electronic Book - Adobe Flash Player required).

https://www.researchgate.net/publication/332901202_Catalogo_de_los_efectos_geologicos_de_los_terremotos_en_Espana_2_Edicion_Revisada_y_ampliada (Pdf version).

The supplementary material for this article provides an original kmz file with the location and brief description (in Spanish) of EEE data in Spain, Europe, Africa and Atlantic Ocean. Due to the scarce availability for exact location and individual descriptions for Portuguese data, this supplementary material study only includes the more significant tsunami sites for Portugal.

Declaration of competing interest

The authors declare that they have no known competing financial interests or personal relationships that could have appeared to influence the work reported in this paper.

Acknowledgments

This work was supported by the Spanish Research Project MINECO-FEDER CGL2015-67169-P (QTECSPAIN - USAL). It is a contribution of the Earthquake Geology Group (TPPT) of the INQUA TERPRO Commission. Authors are grateful to the constructive comments of Joao Fonseca and an anonymous reviewer who significantly improved the content of this paper.

Appendix A. Supplementary data

Supplementary data associated with this article can be found, in the online version, at https://doi.org/10.1016/j.quaint.2021.11.006.

References

Allen, T.I., Hayes, G.P., 2017. Alternative rupture-scaling relationships for subduction interface and other offshore environments. Bull. Seismol. Soc. Am. 107 (3), 1240–1253.

Andrade, C., 1992. Tsunami generated forms in the Algarve barrier islands (south Portugal). Sci. Tsunami Hazards 10 (1), 21–34.

Baptista, M.A., Miranda, P.M.A., Miranda, J.M., Mendes-Vitor, L., 1998. Constrains on the source of the 1755 Lisbon Tsunami inferred from numerical modelling on historical data on the source of the 1755 Lisbon Tsunami. J. Geodyn. 25 (2), 159–174.

Baptista, M.A., Miranda, J.M., Chierici, F., Zitellini, N., 2003. New study of the 1755 earthquake source based on multi-channel seismic survey data and tsunami modeling. Nat. Hazards Earth Syst. Sci. 3, 333–340.

Baptista, M.A., Miranda, J.M., Omira, R., Antunes, C., 2011. Potential inundation of Lisbon downtown by a 1755-like tsunami. Nat. Hazards Earth Syst. Sci. 11, 3319–3326.

Blanc, P.-L., 2009. Earthquakes and tsunami in November 1755 in Morocco: a different reading of contemporaneous documentary sources. Nat. Hazards Earth Syst. Sci. 9, 725–738.
Boore, D.M., Joyner, W., Fumal, T., 1997. Equations for estimating horizontal response spectra and peak acceleration from Western North American earthquakes: a Summary of recent Work. Seismol Res. Lett. 68 (1), 128–153.
Borges, J.F., Fitas, A.J.S., Bezzeghoud, M., Teves-Costa, P., 2001. Seismotectonics of Portugal and its adjacent Atlantic area. Tectonophysics 337, 373–387.
Bufforn, E., López-Sánchez, C., Lozano, L., Martínez Solares, J.M., Cesca, S., Oliveira, C. S., Udías, A., 2020. Re-evaluation of seismic intensities and relocation of 1969 Saint Vincent Cape seismic Sequence: a comparison with the 1755 Lisbon earthquake. Pure Appl. Geophys. 177, 1781–1800.
Buforn, E., Bezzeghoud, M., Udías, A., Pro, C., 2004. Seismic sources on the Iberia-African plate boundary and their tectonic implications. Pure Appl. Geophys. 161, 623–646.
Capote, R., De Vicente, G., González-Casado, J.M., 1991. An application of the slip model of brittle deformation to focal mechanism analysis in three different plate tectonics situations. Tectonophysics 191, 399–409.
Costa, P.J.M., 2016. Imprints of the AD 1755 tsunami in Algarve (south Portugal) lowlands and post-impact recovery. Tsunamis and earthquakes in coastal environments. Springer international publishing, 17–30.
Costa, P.J.M., Dawson, S., Ramalho, R.S., Engel, M., Dourado, F., Bosnic, I., Andrade, C., 2021. A review on onshore tsunami deposits along the Atlantic coasts. Earth Sci. Rev. 212, 103441.
De Vicente, G., Cloetingh, S., Muñoz-Martín, A., Olaiz, A., Stich, D., Vegas, R., Galindo-Zaldivar, J., Fernández-Lozano, J., 2008. Inversion of moment tensor focal mechanisms for active stresses around the microcontinent Iberia: tectonic implications. Tectonics 27, 33–40.
Duarte, J.C., Rosas, F.M., Terrinha, P., Gutscher, M.-A., Malavieille, J., Silva, S., Matias, L., 2011. Thrust-wrench interference tectonics in the Gulf of Cadiz (Africa-Iberia plate boundary in the North-East Atlantic): insights from analog models. Mar. Geol. 289, 135–149.
Duarte, J.C., Rosas, F.M., Terrinha, P., Schellart, W.P., Boutelier, D., Gutscher, M.-A., Ribeiro, A., 2013. Are subduction zones invading the Atlantic? Evidence from the southwest Iberia margin. Geology 41 (8), 839–842.
Duarte, J.C., Schellart, W.P., Rosas, F.M., 2018. The future of Earth's oceans: consequences of subduction initiation in the Atlantic and implications for supercontinent formation. Geol. Mag. 155, 45–58.
Esposito, E., Pece, R., Porfido, S., Tranfaglia, G., 2001. Hydrological anomalies connected to earthquakes in southern Apennines(Italy). Nat. Hazards Earth Syst. Sci. 1, 137–144.
Fonseca, J.B., 2020. A reassessment of the magnitude of the 1755 Lisbon earthquake. Bull. Seismol. Soc. Am. 110, 1–17.
Fontseré, E., 1918. Notas sueltas de sismología Balear» Revista de la Facultad de Ciencias. Universidad de Barcelona, Spain, 12 pp.
Galindo, I., Romero, C., Martín-González, E., Vegas, J., Sánchez, N., 2021. A review on historical tsunamis in the canary islands: implications for tsunami risk reduction. Geosciences 11, 222.
Giner-Robles, J.L., Pérez-López, R., Rodríguez-Pascua, M.A., Martínez-Díaz, J.J., González-Casado, J.M., 2009. Present-day strain field on the South American slab underneath the Sandwich Plate (Southern Atlantic Ocean): a kinematic model: Geological Society London Special Publication 328 (1), 155–167.
Gómez-Diego, P.V., 2016. Análisis Geomático y Catalogación de los Efectos Geológicos y Ambientales del terremoto de Lisboa de 1755 AD. Trabajo Fin de Grado Geomática y Topografía, USAL, 319 p.
Gràcia, E., Vizcaino, A., Escutia, C., Asioli, A., Rodés, A., Pallás, R., Garcia-Orellana, J., Lebreiro, S., Goldfinger, C., 2010. Holocene earthquake record offshore Portugal (SW Iberia): testing turbidite palaeoseismology in a slow-convergence margin. Quat. Sci. Rev. 29, 1156–1172.
Grandin, R., Borges, J.F., Bezzeghoud, M., Caldeira, F., Carrilho, F., 2007. Simulations of strong ground motion in SW Iberia for the 1969 February 28 (MS= 8.0) and the 1755 November 1 (Mw 8.5) earthquakes–II. Strong ground motion simulations. Geophys. J. Int. 171 (2), 807–822.
Gutscher, M.A., Malod, J., Rehault, J.-P., Contrucci, I., Klingelhoefer, F., Mendes-Victor, L., Spakman, W., 2002. Evidence for active subduction beneath Gibraltar. Geology 30 (12), 1071–1074.
Gutscher, M.A., Baptista, M.A., Miranda, J.M., 2006. Constraints on a shallow east dipping fault plane source for the 1755 Lisbon earthquake provided by tsunami modeling and seismic intensity (part 2). Tectonophysics 426, 153–166.
Gutscher, M.A., Dominguez, S., Westbrook, G.K., Le Roy, P., Rosas, F., Duarte, J.C., Terrinha, P., Miranda, J.M., Graindorge, D., Gailler, A., Sallares, V., Bartolome, R., 2012. The Gibraltar subduction: a decade of new geophysical data. Tectonophysics 574, 72–91.
Heidbach, O., Rajabi, M., Cui, X., Fuchs, K., Müller, B., Reinecker, J., Reiter, K., Tingay, M., Wenzel, F., Xie, F., Ziegler, M.O., Zoback, M.-L., Zoback, M.D., 2018. The World Stress Map database release 2016: crustal stress pattern across scales. Tectonophysics 744, 484–498.
Johnston, A.C., 1996. Seismic moment assessment of earthquakes in stable continental regions—III. New Madrid 1811–1812, Charleston 1886 and Lisbon 1755. Geophys. J. Int. 126, 314–344.
Koketsu, K., Yokota, Y., Nishimura, N., Yagi, Y., Miyazaki, S., Satake, K., Fujii, Y., Miyake, H., Sakai, S., Yamanaka, Y., Okada, T., 2012. A unified source model for the 2011 Tohoku earthquake. Earth Planet Sci. Lett. 310, 480–487.
Kvale, A., 1955. Seismic seiches in Norway and England during the Assam earthquake of august 15th, 1950. Bull. Seismol. Soc. Am. 45 (2), 93–113.
Lario, J., Bardají, T., Silva, P.G., Zazo, C., Goy, J.L., 2016. Improving the coastal record of tsunamis in the ESI-07 scale: tsunami Environmental Effects Scale (TEE-16 scale). Geol. Acta 14 (2), 179–193.
Levret, A., 1991. The effects of the November 1, 1755 "Lisbon" earthquake in Morocco. Tectonophysics 193, 83–94.
Luque, L., Lario, J., Zazo, C., Goy, J.L., Dabrio, C.J., Silva, P.G., 2001. Tsunami deposits as paleoseismic indicators: examples from the Spanish coast. Acta Geol. Hisp. 36 (3), 197–211.
Luque, L., Lario, J., Zazo, C., Goy, J.L., Dabrio, C.J., Borja, F., 2002. Sedimentary record of historical tsunamis in the Bay of Cadiz (Spain). J. Quat. Sci. 17, 623–631.
Martínez Solares, J.M., 2001. Los efectos en España del terremoto de Lisboa (1 de noviembre de 1755). Monografías IGN 19. Instituto Geográfico Nacional, Madrid (Spain), 756 pp.
Martínez Solares, J.M., 2017. El Terremoto de Lisboa de 1 de noviembre de 1755. Física Tierra 29, 47–60.
Martínez Solares, J.M., López Arroyo, A., 2004. The great historical 1755 earthquake, effects and damage in Spain. J. Seismol. 8, 275–294.
Martínez-Loriente, S., Sallares, V., Gràcia, E., 2021. The Horseshoe Abyssal Plain Thrust could be the source of the 1755 Lisbon earthquake and tsunami. Springer Nature, Communications Earth & Environment 2.
Martínez-Loriente, S., Sallarès, V., Gràcia, E., Bartolome, R., Dañobeitia, J.J., Zitellini, N., 2014. Seismic and gravity constraints on the nature of the basement in the Africa-Eurasia plate boundary: new insights for the geodynamic evolution of the SW Iberian margin. J. Geophys. Res. Solid Earth 119, 127–149.
Martínez Solares, J.M., Mezcua, J., 2002. Catálogo sísmico de la Península Ibérica (880 a. C. - 1900). *Monografía IGN*, 18. Instituto Geográfico Nacional, Madrid, 253 pp.
Martínez-Loriente, S., Gràcia, E., Bartolome, R., Perea, H., Klaeschen, D., Dañobeitia, J. J., Zitellini, N., Wynn, R.B., Masson, D.B., 2018. Morphostructure, tectono-sedimentary evolution and seismic potential of the Horseshoe fault, SW iberian margin. Basin Res. 30 (1), 382–400.
Mendes-Victor, L., Oliveira, C., Azevedo, J., Ribeiro, A., 2010. The 1755 Lisbon Earthquake: Revisited. Springer., Berlin, Germany, 597 pp.
Michetti, A.M., Esposito, E., Guerrieri, L., Porfido, S., Serva, L., Tatevossian, R., Vittori, E., Audemard, F., Azuma, T., Clague, J., Comerci, V., Gurpinar, A., McCalpin, J., Mohammadioun, B., Morner, N.A., Ota, Y., Roghozin, E., 2007. Intensity scale ESI 2007.Memorie descrittive della Carta Geologica d'Italia, 74, 11–20.
Morales, J.A., Borrego, J., San Miguel, E.G., López-González, N., Caro, B., 2008. Sedimentary record of recent tsunamis in the Huelva Estuary (southwestern Spain). Quat. Sci. Rev. 27 (7–8), 734–746.
Muir-Wood, R., King, G.C.P., 1993. Hydrological signatures of earthquake strain. J. Geophys. Res. 98 (B12), 22035–22068.
Mukherjee, S.M., 1955. Lisbon earthquake of 1 november 1755. Indian J. Meteorol. Geophys. 6 (2), 149–158.
Müller, B., Zoback, M.L., Fuchs, K., Mastin, L., Gregersen, S., Pavoni, N., Stephansson, O., Ljunggren, C., 1992. Regional patterns of tectonic stress in Europe. J. Geophys. Res. 97, 11783–11803.
Navareño Mateos, A., 1982. Arquitectura y urbanismo de Coria: Siglos XVI-XIX. Cáceres, Spain. In: Institución Cultural El Brocense, Diputación De Cáceres, 252 pp.
Olaiz, A.J., Muñoz-Martín, A., De Vicente, G., Vegas, R., Cloetingh, S., 2009. European continuous active tectonic strain–stress map. Tectonophysics 474, 33–40.
Oliveira, C.S., 2008. Review of the 1755 Lisbon earthquake based on recent analyses of historical observations. In: Julien, F., Meghraoui, M., Stucchi, M. (Eds.), Historical Seismology. Modern Approaches in Solid Earth Sciences, pp. 261–300, 2.
Peláez, J.A., Chourak, M., Tadili, B.A., Aït Brahim, L., Hamdache, M., López Casado, J. M., Martínez Solares, J.M., 2007. A catalog of main Moroccan earthquakes from 1045 to 2005. Seismol Res. Lett. 78 (6), 614–621.
Pérez-López, R., Giner-Robles, J.L., Rodríguez-Pascua, M.A., Silva, P.G., Roquero, E., Bardají, T., Elez, J., Huerta, P., 2019. Lichenometric dating of coseismic rockfall related to the Great Lisbon Earthquake in 1755 affecting the archaeological site of "Tolmo de Minateda" (Spain). Z.F. Geomorphologie 62, Suppl. 2, 271–293.
Pintor, Jiménez J., Azor, A., 2006. El Deslizamiento de Güevéjar (provincia de Granada): un caso de inestabilidad de laderas inducida por sismos. Geogaceta 40, 287–290.
Porfido, S., Alessio, G., Gaudiosi, G., Nappi, R., 2020. New perspectives in the definition/evaluation of seismic hazard through analysis of the environmental effects induced by earthquakes. Geosciences, 10 58.
Pro, C., Buforn, E., Bezzeghoud, M., Udías, A., 2013. The earthquakes of 29 july 2003, 12 february 2007, and 17 december 2009 in the region of Cape Saint Vincent (SW Iberia) and their relation with the 1755 Lisbon earthquake. Tectonophysics 583, 16–27.
Reicherter, K., Vonberg, D., Koster, B., Fernández-Steeger, T., Grützner, C., Mathes-Schmidt, M., 2010. The sedimentary inventory of tsunamis along the southern Gulf of Cadiz (southwestern Spain). Zeitschrift für Geomorphologie Suppl. Bd 54 (3), 147–173.
Reid, H.F., 1914. The Lisbon earthquake of november 1, 1755. Bull. Seismol. Soc. Am. 4 (2), 53–80.
Ribeiro, A., Mendes-Victor, L., Cabral, J., Matias, L., Terrinha, P., 2006. The 1755 Lisbon earthquake and the beginning of closure of the Atlantic. Eur. Rev. 14 (2), 193–205.
Robertson, J., Carteret Webb, P., Swithin, A., Hodgson, J., et al., 1755. An extraordinary and Surprising agitation of the waters, though without any perceptible motion of the earth, having been observed in various parts of this island. Phil. Trans. Roy. Soc. Lond. 49, 351–398.
Rodríguez-Pascua, M.A., Silva, P.G., Garduño-Monroy, V.H., Pérez-López, R., Israde-Alcántara, I., Giner-Robles, J.L., Bischoff, J.L., Calvo, J.P., 2010. Ancient earthquakes from archaeoseismic evidence during the Visigothic and Islamic periods in the archaeological site of "Tolmo de Minateda" (SE Spain). In: Sintubin, M.,

Stewart, I.S., Niemi, T.M., Altunel, E. (Eds.), Ancient Earthquakes. Spec. Pap. Geol. Soc. Am., vol. 471, pp. 171–184.
Rodríguez-Vidal, J., Ruiz, F., Cáceres, L.M., Abad, M., González-Regalado, M.L., Pozo, M., Carretero, M.I., Monge-Soares, A.M., Gómez-Toscano, F., 2011a. Geomarkers of the 218-209 BC atlantic tsunami in the roman Lacus Ligustinus (SW Spain): a palaeogeographical approach. Quat. Int. 242, 201–212.
Rodríguez-Vidal, J., Cáceres Puro, L.M., Abad, M., Ruiz Muñoz, F., González-Regalado, Ma L., Finlayson, C., Finlayson, G., Rodríguez Llanes, J.M., 2011b. The recorded evidence of AD 1755 Atlantic tsunami on the Gibraltar coast. J. Iber. Geol. 37 (2), 177–193.
Sallarès, V., Martínez-Loriente, S., Prada, M., Gràcia, E., Ranero, C.R., Gutscher, M.A., Bartolome, R., Gailler, A., Dañobeitia, J.J., Zitellini, N., 2013. Seismic evidence of exhumed mantle rock basement at the Gorringe Bank and the adjacent Horseshoe and Tagus abyssal plains (SW Iberia). Earth Planet Sci. Lett. 365, 120–131.
Sánchez, J.J., Maldonado, R.F., 2016. Application of the ESI 2007 scale to two large earthquakes: south island, New Zealand (2010 Mw 7.1), and Tohoku, Japan (2011 Mw 9.0). Bull. Seismol. Soc. Am. 106 (3), 1151–1161.
Santos, A., Koshimura, S., 2015. The historical review of the 1755 Lisbon tsunami. Journal of Geodesy and Geomatics Engineering 1, 38–52.
Sanz de Ojeda, A., Alhama, I., Sanz, E., 2019. Aquifer Sensitivity to earthquakes: the 1755 Lisbon earthquake. J. Geophys. Res. 124, 8844–8866.
Serra, C.S., Gràcia, E., Bartolome, R., Martínez-Loriente, S., Perea, H., Lo Iacomo, C., Sallarès, V., Urgeles, R., 2018. Hazard in the Gulf of Cadiz: review of the large seismogenic structures. Abstracts Iberfault 3, 321–324.
Serva, L., Vittori, E., Comerci, V., Esposito, E., Guerrieri, L., Michetti, A.M., Mohammadioun, B., Mohammadioun, G.C., Porfido, S., Tatevossian, R.E., 2016. Earthquake hazard and the environmental seismic intensity (ESI) scale. Pure Appl. Geophys. 173 (5), 1479–1515.
Silva, P.G., Rodríguez-Pascua, M.A., 2016. Peligrosidad y riesgo Sísmico: los Terremotos. In: Lario, J., Bardají, T. (Eds.), Introducción a Los Riesgos Geológicos. España, Madrid, pp. 57–113. UNED, Colección Grado.
Silva, P.G., Michetti, A.M., Guerrieri, L., 2015. Intensity scale ESI 2007 for assessing earthquake intensities. In: Beer, M., Kougioumtzoglou, I., Patelli, E., Au, I.K. (Eds.), Encyclopedia of Earthquake Engineering. Springer, Berlin, Heidelberg. https://doi.org/10.1007/978-3-642-36197-5_31-1.
Silva, S., Terrinha, P., Matias, L., Duarte, J.C., Roque, C., Ranero, C.R., Geissler, W.H., Zitellini, N., 2017. Micro-seismicity in the Gulf of Cadiz: is there a link between micro-seismicity, high magnitude earthquakes and active faults? Tectonophysics 717, 226–241.
Silva, P.G., Elez, J., Giner-Robles, J.L., Gómez-Diego, P.V., Rodríguez-Pascua, M.A., Roquero, E., Martínez-Graña, A., Bardají, T., 2017a. The AD 1755 Lisbon Earthquake-Tsunami: modeling the seismic source from the analysis of environmental and building macroseismic data. GNS Science Miscellaneous Series 110, 358–361.
Silva, P.G., Elez, J., Giner-Robles, J.L., Rodríguez-Pascua, M.A., Pérez-López, R., Roquero, E., Bardají, T., Martínez-Graña, A.M., 2017b. ESI-07 ShakeMaps for instrumental and historical events in the Betic Cordillera (SE Spain). Quat. Int. 451, 185–208.
Silva, P.G., Rodríguez-Pascua, M.A., Giner-Robles, J.L., Pérez-López, R., García-Tortosa, F.J., Gómez-Diego, P.V., Bardají, T., Perucha, M.A., Huerta, P., Lario, J., Elez, J., Bautista Davila, B., 2019a. *Catálogo de los Efectos Geológicos de los Terremotos de España, 2ª*. In: *Revisada Y Ampliada*. Serie Riesgos Geológicos Y Geotecnia, 6. IGME, Madrid, Spain, 804 pp.
Silva, P.G., Rodríguez-Pascua, M.A., Giner-Robles, J.L., Elez, J., Pérez-López, R., Bautista Davila, B., 2019b. Catalogue of the geological effects of earthquakes in Spain based on the ESI-07 macroseismic scale: a new database for seismic hazard analysis. Geosciences 9, 334.
Silva, P.G., Elez, J., Giner-Robles, J.L., Pérez-López, R., Roquero, E., Rodríguez-Pascua, M.A., 2020. Reappraisal of the 1863 huércal-overa earthquake (betic Cordillera, SE Spain) by the analysis of ESI-07 environmental effects and building oriented damage. Geosciences 10, 303.
Stich, D., Mancilla, F.L., Pondrelli, S., Morales, J., 2007. Source analysis of the february 12th 2007, Mw 6.0 Horseshoe earthquake: implications for the 1755 Lisbon earthquake. Geophys. Res. Lett. 34, L12308.
Vaz, T., Zêzere, J.L., 2016. Landslides and other geomorphologic and hydrologic effects induced by earthquakes in Portugal. Nat. Hazards 81 (1), 71–98.
Vilanova, S.P., Nunes, C.F., Fonseca, J.F., 2003. Lisbon 1755: a case of triggered onshore rupture? Bull. Seismol. Soc. Am. 93 (5), 2056–2068.
Wald, D.J., Worden, B.C., Quitoriano, V., Pankow, K.L., 2005. ShakeMap manual: technical manual, user's Guide, and software Guide. U.S. Geological survey, p. 132.
Wang, M., Li, Q., Wang, F., Zhang, R., Wang, Y.Z., Shi, H.B., Zhang, P.Z., Shen, Z.K., 2011. Far-field coseismic displacements associated with the 2011 Tohoku-oki earthquake in Japan observed by Global Positioning System. Chin. Sci. Bull. 56, 2419–2424.
Wang, D., Mori, J., Uchide, T., 2012. Supershear rupture on multiple faults for the Mw 8.6 off northern Sumatra, Indonesia earthquake of april 11, 2012. Geophys. Res. Lett. 39, L21307.
Yamaguchin, A., Mori, T., Kazama, M., Yoshida, N., 2012. Liquefaction in Tohoku district during the 2011 off the pacific coast of Tohoku earthquake. Soils Found. 52 (5), 811–829.
Zitellini, N., Mendes Victor, L.A., Cordoba, J.D., Dañobeitia, J., Nicolich, R., Pellis, G., Ribeiro, A., Sartori, R., Torelli, L., Bartolome, R., et al., 2001. Source of 1755 Lisbon earthquake and tsunami investigated. EOS Transactions 82 (26), 285.
Zitellini, N., Gracia, E., Matias, L., Terrinha, P., Abreu, M.A., De Alteriis, G.J., Henriet, P., Dañobeitia, J.J., Masson, D.G., Mulder, T., Ramella, R., Somoza, L., Diez, S., 2009. The quest for the Africa-Eurasia plate boundary west of the Strait of Gibraltar. Earth Planet Sci. Lett. 280 (1/4), 13–50.